(12) INTERNATIONAL APPLICATION PUBLISHED UNDER THE PATENT COOPERATION TREATY (PCT)

(19) World Intellectual Property Organization
International Bureau

(43) International Publication Date
17 September 2020 (17.09.2020)

WIPO | PCT

(10) International Publication Number
WO 2020/183215 A1

(51) International Patent Classification:
H01M 2/14 (2006.01) *H01M 2/16* (2006.01)

(21) International Application Number:
PCT/IB2019/000452

(22) International Filing Date:
14 March 2019 (14.03.2019)

(25) Filing Language: English

(26) Publication Language: English

(71) Applicants: **SORBONNE UNIVERSITÉ** [FR/FR]; 21 rue de l'Ecole de Médecine, 75006 Paris (FR). **COLLEGE DE FRANCE** [FR/FR]; 11 place Marcelin Berthelot, 75005 Paris (FR). **CENTRE NATIONAL DE LA RECHERCHE SCIENTIFIQUE** [FR/FR]; 3, rue Michel Ange, 75016 Paris (FR).

(72) Inventors: **COUSTAN, Laura**; 44, rue de la Clef, 75005 Paris (FR). **LABERTY-ROBERT, Christel**; 26, rue Berthollet, 75005 Paris (FR). **TARASCON, Jean-Marie**; 54 rue Boissonade Escalier A, 75014 Paris (FR).

(74) Agent: **HABASQUE, Etienne** et al.; Lavoix, 2, place d'Estienne d'Orves, 75441 Paris Cedex 09 (FR).

(81) Designated States *(unless otherwise indicated, for every kind of national protection available)*: AE, AG, AL, AM, AO, AT, AU, AZ, BA, BB, BG, BH, BN, BR, BW, BY, BZ, CA, CH, CL, CN, CO, CR, CU, CZ, DE, DJ, DK, DM, DO, DZ, EC, EE, EG, ES, FI, GB, GD, GE, GH, GM, GT, HN, HR, HU, ID, IL, IN, IR, IS, JO, JP, KE, KG, KH, KN, KP, KR, KW, KZ, LA, LC, LK, LR, LS, LU, LY, MA, MD, ME, MG, MK, MN, MW, MX, MY, MZ, NA, NG, NI, NO, NZ, OM, PA, PE, PG, PH, PL, PT, QA, RO, RS, RU, RW, SA, SC, SD, SE, SG, SK, SL, SM, ST, SV, SY, TH, TJ, TM, TN, TR, TT, TZ, UA, UG, US, UZ, VC, VN, ZA, ZM, ZW.

(84) Designated States *(unless otherwise indicated, for every kind of regional protection available)*: ARIPO (BW, GH, GM, KE, LR, LS, MW, MZ, NA, RW, SD, SL, ST, SZ, TZ, UG, ZM, ZW), Eurasian (AM, AZ, BY, KG, KZ, RU, TJ, TM), European (AL, AT, BE, BG, CH, CY, CZ, DE, DK, EE, ES, FI, FR, GB, GR, HR, HU, IE, IS, IT, LT, LU, LV, MC, MK, MT, NL, NO, PL, PT, RO, RS, SE, SI, SK, SM, TR), OAPI (BF, BJ, CF, CG, CI, CM, GA, GN, GQ, GW, KM, ML, MR, NE, SN, TD, TG).

Published:
— *with international search report (Art. 21(3))*

WO 2020/183215 A1

(54) Title: SEPARATOR, PROCESS FOR MANUFACTURING SAID SEPARATOR AND SODIUM ION BATTERIE COMPRISING SAID SEPARATOR

(57) Abstract: The present invention relates to a battery separator comprising monophasic non- woven hybrid nanofibers, wherein: - said non-woven hybrid nanofibers comprise at least one metal oxide and at least one polymer chosen from the group consisting of fluoropolymers, vinylpolymers, polyethers, and mixtures thereof, and - said non-woven hybrid nanofibers have a diameter ranging from 20 to 1,000 nm.

SEPARATOR, PROCESS FOR MANUFACTURING SAID SEPARATOR AND SODIUM ION BATTERIE COMPRISING SAID SEPARATOR

The present invention concerns a separator for battery, in particular for sodium-ion battery, and a process for manufacturing said separator.

The present invention also concerns a sodium-ion battery comprising such separator.

In a battery, the microporous structure and thermal dimensional stability of the separator that isolates the two electrodes considerably affect the battery performances, including power densities, cycle life and safety characteristics. This has led to the design of separators that possess high ion conductivity, mechanical properties together with a wide electrochemical stability at room temperature. Currently, the trilayer PP-PE-PP microporous separators (commercially available as Celgard®) are the most widely used separators for sodium-ion (Na-ion) batteries due to their advantages, such as good electrochemical stability, proper thickness, and considerable mechanical strength. However, these separators often suffer from poor electrolyte wettability and severe dimensional instability at elevated operating temperature, i.e. when the battery is operated at high charge/discharge current.

A modification of the surface by a thin layer (20 nm) of ceramic nanoparticles as TiO_2, Al_2O_3 or SiO_2 has been proposed by Etacheri et al. (*Energy Environ. Sci.,* 4 (2011), 3243-3262) to circumvent the wettability issue and eventual dendrites growth, but sometimes to the expense of the battery rate capability, owing to the added interface resistance. More importantly, the processing of this separator is complex as it includes successive tape casting layers made of polymer and ceramics.

Cui et al. (*ACS Appl. Mater. Interfaces*, 5 (2013), 128-134) discloses renewable, low cost and environmentally benign cellulose/poly(vinylidene fluoride-co-hexafluoropropylene) composite non-woven separator as an advanced separator for high-performance lithium-ion battery via a two-steps process including electrospinning and dip-coating. However, a drawback pertaining to cellulose is its highly flammability, which is prejudicial for safety concern when sodium-ion batteries are abused.

There is thus still a need of an improved battery separator which could alleviate the above limitations.

Thus, the aim of the present invention is to provide a battery separator with improved properties, and more particularly with an improved wettability and an important electrolyte uptake with little dimension changes.

The aim of the present invention is also to provide a battery separator for sodium-ion battery with improved performances, and more particularly a high capacity rate.

Another aim of the invention is to provide a battery separator for sodium-ion battery with high safety properties.

Therefore, the present invention relates to a battery separator comprising monophasic non-woven hybrid nanofibers, wherein said non-woven hybrid nanofibers comprise at least one metal oxide and at least one polymer chosen from the group consisting of fluoropolymers, vinylpolymers, polyethers, and mixtures thereof, and wherein said non-woven hybrid nanofibers have a diameter ranging from 20 to 1,000 nm, preferably ranging from 50 to 500 nm, more preferably ranging from 115 to 175 nm.

According to the present invention, the monophasic non-woven hybrid nanofibers are constituted of alternated domains of metal oxide and a domain of polymer intimately mixed at the nanometer scale, resulting in an absence of phase separation at the micron level. Metal oxide domains are dispersed into the polymer domain.

The non-woven hybrid nanofibers according to the invention may also be named as composite nanofibers.

According to the present invention, the term “non-woven nanofibers” means that the nanofibers are not interlinked but are free and can move to each other. The nanofibers of the present invention are intermingled, randomly organized into 3-D direction and delineate a continuous highly porous network.

The presence of metal oxide intimately mixed with the polymer improves the wettability of separator with various electrolytes and increases electrolyte uptake. The high porosity and high wettability facilitate the diffusion/migration of ions throughout the electrolyte, thus improving the capacity rate.

The high porosity also prevents the separator to swell upon electrolyte uptake.

In addition, the separator according to the invention is safer compared to standard commercial separators. The non-woven nanofibers of the battery separator according to the present invention limit dendrite sodium growth as compared to standard commercial separator (as alumina coated PEO), then extending short circuit time and preventing battery explosion. Also, the presence of metal oxide intimately mixed with the polymer decreases the separator flammability compared to standard commercial separators.

The battery separator according to the present invention may be self-supported, which means that the battery separator can be used without any mechanical support.

According to an embodiment, the metal oxide is selected from the group consisting of SiO_2, Al_2O_3, ZrO_2, TiO_2, and mixtures thereof. Preferably, the metal oxide is SiO_2.

According to an embodiment, the polymer is chosen from the group consisting of polyvinylidene fluoride (PVDF), polyvinylidene fluoride-hexafluoropropylene (PVDF-HFP), polyethylene oxide (PEO), polyvinylpyrrolidone (PVP), polyvinyl alcohol (PVA), and mixtures thereof. Preferably, the polymer is polyvinylidene fluoride-hexafluoropropylene.

According to an embodiment, the metal oxide content ranges from 5% to 70% by weight, preferably from 30% to 50% by weight, more preferably from 35% to 45% by weight in relation to the total weight of non-woven hybrid nanofibers. Advantageously, the metal oxide content is equal to 40% by weight with regard to the total weight of non-woven hybrid nanofibers.

According to an embodiment, the polymer content ranges from 30% to 95% by weight, preferably from 50% to 70% by weight, more preferably from 55% to 65% by weight in relation to the total weight of non-woven hybrid nanofibers. Advantageously, the polymer content is equal to 60% by weight in relation to the total weight of non-woven hybrid nanofibers.

According to an embodiment, the battery separator of the present invention has a thickness ranging from 10 µm to 100 µm, preferably ranging from 10 µm to 50 µm, more preferably ranging from 15 µm to 25 µm.

According to an embodiment, the battery separator of the present invention has a porosity ranging from 10% to 90% by volume, preferably ranging from 50% to 90% by volume, more preferably ranging from 80% to 90% by volume in relation to the total volume of the battery separator.

According to an embodiment, the battery separator of the present invention has an electrolyte uptake capacity ranging from 100% to 600% by weight, preferably ranging from 140% to 550% by weight, more preferably ranging from 510% to 550% by weight in relation to the weight of the battery separator before impregnation with the electrolyte.

According to the present invention, the term “electrolyte uptake capacity” of a battery separator relates to the capacity of said battery separator to absorb a liquid electrolyte. This capacity is assessed by comparison of the weight of the battery separator before and after electrolyte absorption.

The present invention also relates to a process for manufacturing the battery separator of the invention, said process coupling a sol-gel reaction and an electrospinning method, comprising the following steps:

i) preparing a mixture comprising at least one polymer as defined above, and one metal precursor, said metal precursor being a metal alkoxide chosen from the group consisting of silicon alkoxide, titanium alkoxide, zirconium alkoxide and aluminum alkoxide,

ii) electrospinning the mixture obtained at the end of step i) by applying a positive voltage to said mixture for obtaining a material deposited onto a support, and

iii) drying the deposited material obtained at the end of step ii) and removing the support to obtain the battery separator.

The coupling of sol-gel chemistry and electrospinning method enables the manufacturing of the monophasic non-woven hybrid nanofibers comprised in the battery separator of the invention. During the process of the invention, the sol-gel reaction, occurring during both steps i) and ii), leads to the formation of the metal oxide domains. The electrospinning method applied during step ii) enables the formation of the non-woven hybrid nanofibers comprised in the battery separator.

These hybrid nanofibers are non-woven due to the electrospinning method of the process according to the invention, whereas the absence of phase separation in the non-woven hybrid nanofibers comprised in the battery separator is due to the coupling of sol-gel chemistry and electrospinning method.

The process of the invention is low cost and easily scalable.

According to the invention, a “metal precursor” is a chemical metallic compound participating in a sol-gel reaction for the production of a material comprising at least one metal oxide.

According to an embodiment, the metal precursor of step i) of the process according to the invention is chosen from the group consisting of tetraethyl orthosilicate, titanium tetraisopropoxide, zirconium tetraisopropoxide, aluminium isopropoxide and mixtures thereof. Preferably, the metal precursor is tetraethyl orthosilicate.

According to an embodiment, the mixture of step i) of the process according to the invention is prepared in a solvent chosen from the group consisting of N,N-

dimethylformamide, ethanol, tetrahydrofuran, and mixtures thereof. Preferably, the mixture of step i) is prepared in N,N-dimethylformamide.

According to an embodiment, the positive voltage applied during step ii) of the process according to the invention is comprised between 5 kV and 25 kV. Preferably, the positive voltage applied during step ii) is equal to 18 kV.

According to an embodiment, the mixture of step i) of the process of the invention comprises from 2% to 40% by weight, preferably from 5% to 25% by weight, more preferably 10% by weight of the polymer in relation to the total weight of the solvent.

According to an embodiment, the mixture of step i) of the process of the invention comprises a polymer/metal precursor weight ratio comprised between 3:7 and 95:5 preferably between 3:7 and 7:3. More preferably, the polymer/metal precursor weight ratio in the mixture of step i) is equal to 6:4.

According to an embodiment, the step i) of the process according to the invention is implemented at a temperature comprised between 40°C and 80°C, preferably comprised between 50°C and 70°C, more preferably at 60°C.

According to an embodiment, the step i) of the process according to the invention is implemented during between 8 hours and 24 hours, preferably between 10 hours and 20 hours, more preferably during 12 hours.

According to an embodiment, the step ii) of the process according to the invention is implemented at a feed rate ranging from 0.010 mL/min to 0.040 mL/min, preferably from 0.020 mL/min to 0.030 mL/min, more preferably the feed rate is equal to 0.025 mL/min.

According to an embodiment, the step ii) of the process according to the invention is implemented at a temperature comprised between 20°C and 40°C, preferably comprised between 20°C and 30°C, more preferably at 25°C

According to an embodiment, the step iii) of the process according to the invention is implemented during between 10 hours and 36 hours, preferably between 20 hours and 30 hours, more preferably during 24 hours.

According to an embodiment, the step iii) of the process according to the invention is implemented at a temperature comprised between 50°C and 90°C, preferably comprised between 60°C and 80°C, more preferably at 70°C

According to an embodiment, the support of step (ii) of the process is a metal foil, a cupper foil or a gold foil. Preferably, the support is an aluminum foil.

The present invention also relates to the use of the battery separator as defined above in a Li-ion battery, Na-ion battery or metal-air battery, preferably in a Na-ion battery.

The present invention also relates to a Na-ion battery comprising:

- at least one positive electrode comprising at least one positive electrode active material and a current collector,
- at least one negative electrode comprising a negative electrode active material, and
- at least one battery separator according to the invention, said battery separator being impregnated with at least one electrolyte, said separator being placed between the positive electrode and the negative electrode.

Preferably, the electrolyte impregnated in the separator of the Na-ion battery of the invention comprises at least one solvent and one sodium salt.

According to an embodiment, said solvent is chosen from the group consisting of: ethylene carbonate-dimethyl carbonate (EC-DMC), ethylene carbonate-propylene carbonate (EC-PC)water in salt, and mixtures thereof.

According to an embodiment, said sodium salt is chosen from the group consisting of: sodium hexafluorophosphate ($NaPF_6$), sodium perchlorate ($NaClO_4$), sodium bis (fluorosulfonyl) imide (NaFSI), sodium bis(trifluoromethanesulfonyl)imide (NaTFSI), sodium bis(pentafluoroethanesulfonyl)imide (NaBETI), sodium tetrafluoroborate ($NaBF_4$), and mixtures thereof.

The positive electrode active material is a material capable of inserting sodium ions reversibly which may be chosen among oxides such as Na_xMO_2 in which M represents at least one metallic element selected from the group comprising Ni, Co, Mn, Fe, Cr, Ti, Cu, V, Al and Mg and phosphates such as $NaTi_2(PO_4)_3$, $Na_3V_2(PO_4)_3$, $Na_3V_2(PO_4)_2F_3$, $Na_2MnP_2O_7$, Na_2MnPO_4F, $Na_{1.5}VPO_{4.8}F_{0.7}$ and $NaV_{1-x}Cr_xPO_4F$. Among these positive electrode active materials, $Na_3V_2(PO_4)_2F_3$, also named NVPF, $Na_{2/3}Mg_{1/3}Mn_{2/3}O_2$, and a mixture thereof, are particularly preferred.

In addition to the positive electrode active material, the positive electrode may further include a polymer binder and optionally an electronic conducting agent.

As example of polymer binder, mention may be made of polyvinylidene difluoride (PVdF), poly(tetrafluoroethylene) (PTFE), cellulose fibers, cellulose derivatives such as starch, carboxymethyl cellulose (CMC), diacetyl cellulose, hydroxyethyl cellulose or hydroxypropyl cellulose, styrene butadiene rubber (SBR) and a mixture thereof. Among these binders, PVdF is preferred.

The conductive agent may be carbon black, Super P carbon black, acetylene black, ketjen black, channel black, natural or synthetic graphite, carbon fibers, carbon nanotubes, vapor grown carbon fibers or a mixture thereof.

The weight proportions, relatively to the total weight of the positive electrode, are preferably:

- Positive electrode active material: 80% to 98%
- Electronic conducting agent: 1% to 10%
- Polymer binder: 1% to 10%.

The negative electrode active material used for the negative electrode can be selected among carbon materials, in particular hard carbon, soft carbon, carbon nanofibers or carbon felt, antimony, tin, and phosphorus.

Preferably, the negative electrode active material is a carbon material and said negative electrode further comprises a polymer binder which may be chosen among the same polymer binders as those mentioned above for the positive electrode, and preferably from cellulose derivatives binders.

As mentioned for the positive electrode, the negative electrode may further include a conductive agent which may be chosen among the same conductive agent as those mentioned above for the positive electrode.

The negative electrode may also include a current collector.

The current collectors of the positive and negative electrodes may be composed of a conductive material, more particularly of a metallic material which may be selected from aluminum, copper, nickel, titanium and steel.

A Na-ion battery according to the invention may be composed of a single electrochemical cell comprising two electrodes (i.e. one positive electrode and one negative electrode) separated by a separator according to the invention; or of a plurality of chemical cells assembled in series; or of a plurality of chemical cells assembled in parallel; or of a combination of the two assembly types.

FIGURES

In the following parts, the battery separator according to the invention is also designated as EHS (Electrospun Hybrid Separator).

Figure 1 gives an SEM (Scanning Electron Microscopy) micrograph of a separator according to the invention (Surface (Figure 1A), cross-section (Figure 1B)) and the fiber diameter distribution in the separators according to the invention (Figure 1C).

Figure 2 gives the wettability over time of a separator according to the invention (contact angle wettability images (Figure 2A), surface impregnation images before impregnation (Figure 2B), at time = 0 second (Figure 2C) and time = 10 seconds (Figure 2D) after electrolyte drop deposition of with 1 M $NaPF_6$ in EC/PC (volume ratio 1/1).

Figure 3 gives the capacity retention plot of the $Na_3V_2(PO_4)_2F_3$ (NVPF)// $NaPF_6$-EC:PC// Hard carbon full cells prepared with a separator according to the invention for which cycles are controlled between 2 V and 4.3 V cut off (left) and the electrochemical stability of the electrolyte and a separator according to the invention between 2.5 V and 5 V in a Na// $NaPF_6$-EC:PC// Stainless Steel cell (right).

Figure 4 gives the galvanostatic charge-discharge cycling profile of NVPF electrodes (Figure 4-left), first cycle (solid curves) and fifth cycle (dash curves) and the capacity rate behavior of NVPF electrodes (Figure 4-right).

Figure 5 gives the short circuit time due the dendrite growth measured in a symmetric Na// $NaPF_6$-EC:PC// Na cell with a separator according to the invention by applying a current density of 0.3 mA/cm^2.

Figure 6 gives the morphological and physical properties of two commercial separators (Al_2O_3-coated PE (polyethylene) separator: A and D; cellulose separator: B and E) and of the separator according to the invention (C and F) obtained by scanning electronic microscopy.

Figure 7 gives the contact angle wettability of Al_2O_3-coated PE separator, cellulose separator and separator according to the invention with 1 M $NaPF_6$ in EC/PC (volume ratio 1/1) (contact angle wettability images and surface impregnation images before impregnation, at time = 0 second and time = 10 seconds after electrolyte drop deposition).

Figure 8 gives the DSC (Differential Scanning Calorimetry) analysis of Al_2O_3-coated PE separator, cellulose separator and separator according to the invention.

Figure 9 gives the thermal shrinkage of Al_2O_3-coated PE separator, cellulose separator and separator according to the invention over a temperature range from 70°C to 160°C for 0.5 h at each temperature (left), and their combustion behavior (right).

Figure 10 gives the stress-strain curves of Al_2O_3-coated PE separator, cellulose separator and separator according to the invention in their “dry state” in the transverse direction at room temperature.

Figure 11 gives the first charge (black curve, Q = 83 mAh/g) and discharge (grey curve, Q = 74 mAh/g) curves for NVPF/HC (hard carbon) full cell containing Al_2O_3-coated PE separator.

Figure 12 gives the first charge (black curve, Q = 120 mAh/g) and discharge (grey curve, Q = 99 mAh/g) curves for NVPF/HC (hard carbon) full cell containing cellulose separator.

Figure 13 gives the first charge (black curve, Q = 129 mAh/g) and discharge (grey curve, Q = 108 mAh/g) curves for NVPF/HC (hard carbon) full cell containing separator according to the invention.

Figure 14 gives the capacity rate for NVPF/HC full cell containing Al_2O_3-coated PE separator

Figure 15 gives the capacity rate for NVPF/HC full cell containing cellulose separator.

Figure 16 gives the capacity rate for NVPF/HC full cell containing separator according to the invention.

Figure 17 gives the short circuit time of Al_2O_3-coated PE separator, cellulose separator and separator according to the invention.

Figure 18 gives the voltage curves for NVPF/HC full cell containing Al_2O_3-coated PE separator, cellulose separator and separator according to the invention.

EXAMPLES

Example 1: Preparation of the battery separator of the invention

The materials used for the preparation of separator according to the present invention were poly(vinylidene fluoride-co-hexafluoropropene) (PVDF-HFP) (Solvay), tetraethyl orthosilicate (TEOS) (Sigma-Aldrich, 98% traces of metals), and N,N - dimethylformamide (Sigma-Aldrich). These materials were used as received without further purification.

The electrospinning setup utilized in this study consisted of a syringe and needle (ID = 0.75 mm), a ground electrode and a high voltage supply commercial platform (ES1a, Electrospinz). The needle was connected to the high voltage supply, which could generate positive DC voltages up to 40 kV.

For the preparation of the separator according to the invention, 10% by weight of PVDF-HFP was first dissolved in N,N-dimethylformamide (DMF). The pure precursors sol TEOS were added, mixed at 60°C during few hours toget an homogenous solution with a PDVF-HFP:TEOS ratio of 6:4 in weight (this mass percentage should be kept for the dry membrane). Then, 1.2 mL of the solution was electrospun at 18 kV, 0.025 $mL.min^{-1}$. The steel needle was connected to an electrode of a high voltage supply and a grounded aluminum foil was placed at 15 cm distance from the needle tip to collect the separator. The electrospinning was carried out at room temperature and below 60% relative humidity. A white, flexible material was obtained. Finally, the separator was dried during 24 h at 70°C in air. After the drying, the separator was carefully peeled off from the aluminum foil.

Main characteristics of the separator are gathered in the table below.

The electrolyte uptake of the separator of the invention was estimated by simply measuring its weight gains when placed into (1 M of $NaPF_6$ in EC/PC) electrolyte for 5 minutes. The porosity of the different separators was measured as described by Wu et al. (*Polymer* 46 (2005) 5929–5938) by immersing the membranes in n-butanol and calculated using the following equation:

$$P\,(\%) = {m_1 - m_0}/{\rho V} \cdot 100$$

where m_1 and m_0 are the mass of the absorbed n-butanol and the dry membrane, ρ the density of the n-butanol and V the volume of the polymer). The ionic conductivity was determined through impedance spectroscopy using in symmetrical cell, using blocking

aluminum foil as electrodes. The three separators, have been impregnated by 1 M $NaPF_6$ in EC/PC.

Thickness before impregnation (µm)	Electrolyte uptake (weight %)	Thickness post-impregnation (µm)	Porosity (%)	Ionic conductivity (Electrolyte + Separator) (mS/cm)	Conductivity (Electrolyte) (mS/cm)
18.4 ± 0.8	528 ± 13	15.3 ± 0.6	85.4 ± 0.4	2.78 ± 0.16	8.21

As shown in Figure 1A, the separator of the invention comprises intermingled fibers (D = 130 nm) randomly organized into 3-D direction so as they delineate a continuous porous network of 85.4% with no phase separation at the micron level. The membrane thickness is 18 µm (Figure 1B). This particular structure may explain the interesting properties of wettability of the separator. The diameter of the electrospun fibers of the separator of the invention ranged from 50 nm to 300 nm with diameter average 130 nm. The values were determined from 100 fibers (Figure 1C).

Figure 2 shows the variation of the angle formed between a $NaPF_6$-EC:PC electrolyte drop and the separator and its impregnation time.

When an interface exists between a liquid and a solid, the angle between the surface of the liquid and the outline of the contact surface is described as the contact angle θ. The contact angle (wetting angle) is a measure of the wettability of a solid by a liquid. In the case of complete wetting, the contact angle is 0°. Between 0° and 90°, the solid is wettable and above 90° it is not wettable. In the case of ultrahydrophobic materials, the contact angle approaches the theoretical limit of 180°.

In the case of the separator of the invention, the value of the angle is low and the time for impregnation is quick: few seconds is enough to wet the separator, without need of vacuum treatment. As a consequence, an electrolyte uptake of 528% ± 13% by weight is achieved, accompanied with little modification of the dimension of the separator. In addition, ionic conductivity of the impregnated separator is 2.78 $mS.cm^{-1}$ ± 0.16 $mS.cm^{-1}$ at room temperature, which is close to the one observed for pure EC/PC electrolyte.

Example 2: Electrochemical performances of Na-ion battery containing the battery separator of the invention

The performances of the above-mentioned separator have been tested in Na-ion battery having the following configuration.

The electrochemical performance of the obtained separator was measured in NVPF/HC full cells in $NaPF_6$ (Stella, Japan) 1 molar in EC/PC with 1/1 ratio. The electrochemical performance of NVPF/EHS/HC full cells was evaluated in 2025-type coin cells made of 11 mm NVPF and HC disks, punched from tape casted slurries on Al current collector, and separated by different separators containing 150 µL electrolytes. Electrodes loading of 12 and 6 mg cm-2 were used for NVPF and HC electrodes, respectively, so that the NVPF/HC full cells are designed cathode-limited if not otherwise specified. All of the electrodes and separators were put into a Buchi glass oven at 80 °C under vacuum for 24 h prior to be transferred into glovebox (MBraun MB200B). All cells were galvanostatically cycled by using VMP3 or MPG2 potentiostat (Biologic, France) at room temperature. The capacity is reported with an accuracy of 0.5% $mA.g^{-1}$. It is worth mentioning that the precision of variation in with the cycling rates calculated on the basis of NVPF (1C = 128 capacity of a given cell depends only on the accuracy of the potentiostat (in the order of 0.5%).

Figure 3 shows that at a capacity rate of C/10, the initial discharge capacity of the NVPF// $NaPF_6$-EC:PC// Hard carbon full cells prepared with the separator of the invention is 107.5 mAh/g and is maintained for almost 60 cycles. After 100 cycles, the retention capacity is equal to 98%. The reason for the excellent retention of capacity is linked to the excellent porosity and the electrochemical stability of the separator, enhanced by the presence of SiO_2.

In addition, as shown in Figure 4 (left), the capacity loss for the first cycle is moderate, but after this cycle, the subsequent cycle performance are quite excellent with almost no capacity loss. By looking at the capacity rate behavior (Figure 4, right), it is easy to confirm the optimization of the cell performance, especially in power density. This enhanced behavior compared to the cell studied in the literature may be explained by the excellent wettability and electrolyte uptake verified in the Figure 2, which is directly induced by the non-woven hybrid organic/inorganic nanofibers.

Finally, Figure 5 shows that a huge drop in potential is observed at t = 100 h. The separator according to the invention limits the dendrite growth by blocking and disturbing the dendrite pathway. This has been made possible thanks to the flexible, non-woven nanofibers and the presence of SiO_2. This latter is also well-known to increase the

temperature of material flammability which further improves the safety while ensuring the mechanical strength of the membrane, a must for processing. The presence of the inorganic part and the ability of the nanofibers to hinder the dendrite growth considerably increase the security of the battery.

Example 3: Comparison with commercial battery separators

Al_2O_3 coated single layer polyethylene (PE) separator was kindly provided by the Shenzhen Xuran Electronic Co. From the material data sheet, the reported thickness and porosity of the Al_2O_3-coated PE separator were 16 µm (12 µm of PE and 4 µm of Al_2O_3) and 0.45 ± 5, (45%), respectively.

Cellulose separator manufactured by "DreamWeaver" company was also used to compare with the separator according to the invention. From the material datasheet, the reported thickness and porosity of the cellulose separator were 30 µm and 0.61 (61%), respectively.

Figure 6 exhibits the surface and cross-section of the separator of the invention which consists of randomly arranged hybrid fibers with size of 145 ± 30 nm in diameter (Figure 6C) with pores of a few microns in diameter (Figure 6F) leading to a high tortuous structure. By comparison, the Al_2O_3-coated PE separator (Figures 6A and 6D) is fiber-free and shows an interconnected submicronic pore structure and a thickness of about 16 µm, while the cellulose separator (Figures 6B and 6E) exhibits a thickness of 30 µm and consists of randomly arranged fibers with diameter size of 2 ± 0.2 µm with excessively large-sized pores (> 4 µm). Additionally, the separator of the invention exhibits the highest porosity with a value of 85.4% compared to 42.8% for Al_2O_3-coated PE separator and 49.9% for cellulose separator (see the table below) (note that the porosity of the different separators was measured as described in example 1). In contrast, the tortuosity of the separator of the invention (~15.9%), as deduced from combined porosity and ionic conductivity measurements, was found to be comparable to the one for cellulose and is lower than that of Al_2O_3-coated PE separator. The tortuosity of the different separator was calculated from the values of the porosity thanks to the following equation:

$$T(\%) = \sqrt{P \cdot \left(\sigma_e / \sigma_S\right)} \cdot 100$$

where T is the tortuosity of the separator, P its porosity, σ_e the ionic conductivity of the electrolyte and σ_s the ionic of the electrolyte into the separator).

.

Separator	Porosity (%)	Tortuosity (%)
Al_2O_3 coated PE	42.8 ± 0.4	24.8 ± 0.2
Cellulose	49.9 ± 0.7	12.8 ± 0.4
Separator of the invention	85.4 ± 0.4	15.9 ± 0.5

The wettability was probed by measuring the contact angle between the liquid electrolyte (1 M of $NaPF_6$ in EC/PC) and the separator of the invention (Figure 7) following the method described in Example 1. A contact angle of nearly (~0°) was found and this value is much lower than that of cellulose separator (~30°C) and of Al_2O_3-coated PE separator (~70°C), which confirms that the separator of the invention exhibits better electrolyte wettability than the two other studied separators. This remarkable liquid electrolyte wettability may be ascribed to the very high connected porosity and the intrinsically lyophilic nature of the hybrid fibers. The electrolyte uptake of the separator of the invention was estimated to 528% by weight by measuring its weight gains when placed into (1 M of $NaPF_6$ in EC/PC) electrolyte for 5 minutes. This value is quite higher than those of 123% by weight and 144% by weight measured under similar conditions for the cellulose separator and the Al_2O_3-coated PP separator, respectively (see the table below). In addition, the separator of the invention does not swell upon electrolyte uptake, whereas Al_2O_3-coated PE separator volume increases by 144% after electrolyte impregnation. This is most likely the result of several combined factors including high specific surface area, porosity and the hydrophilic character of the fibers due to the presence of SiO_2.

Separator	Thickening (%)	Electrolyte uptake (%)
Al_2O_3 coated PE	144 ± 15	144 ± 8
Cellulose	30 ± 3	123 ± 2
Separator of the invention	-16 ± 2	528 ± 13

Considering that the safety characteristic of a separator is its shut-down temperature which is associated to the shrinkage/closing of the pores near its melting temperature, the thermal behavior of the commercial separators and the separator of the invention was assessed by Differential Scanning Calorimetry (DSC) analysis (TA Instruments Thermal Analysis System Q20). DSC is a thermoanalytical technique in which the difference in the amount of heat required to increase the temperature of a sample and reference is measured as a function of temperature. During these analyses, the samples were stabilized at -80°C and then heated from -80 °C to 180 °C at 10 °C min^{1} to remove moisture, recooled to - 80 °C, then reheated from that temperature to 250 °C at 10 °C min^{-1} in air.

Thermograms shown in Figure 8 reveal the existence of an intense exothermic peak at 136°C for the Al_2O_3-coated PE separator, which corresponds to the PE melting temperature and to the reported separator shut-down temperature. In contrast, the DSC profile for the separator of the invention exhibits a weak peak of smaller intensity at slightly higher temperature (139°C) that corresponds to the melting point of PVDF-HFP. Lastly, for the cellulose separator, the exothermic peak solely appears at 250°C, as previously reported, implying that this membrane has the greatest thermal stability but is of no use for shutdown applications because of its too high melting temperature.

The thermal shrinkage behavior of these separators was also explored (Figure 9). The separators were placed in an oven at a given temperature and their size was measured after 30 minutes. It was found that cellulose separator exhibits negligible thermal shrinkage when compared to Al_2O_3-coated PE separator and to the separator of the invention, both showing identical behavior, as both curves neatly superimpose. This could suggest that the separator of the invention possesses attractive shutdown properties as commercial Al_2O_3-coated PE separator. Finally, the three separators were benchmarked for their combustion behavior. As it can be viewed in Figure 9B, the flammability is the highest for the cellulose separator, that burst into flame after 5 s, and the lowest for the separator of the invention, which practically remains as such after 15 s, while Al_2O_3-coated PE separator is completely deteriorated after 10 s. Altogether, these results demonstrate the excellent thermal tolerance of the separator of the invention.

A Dynamic Mechanical Analyzer (DMA, TA Instruments Thermal Analysis System Q800, New Castle, DE) was used to obtain the mechanical behavior of the separator, by applying a constant displacement of 1 mm/min, to breakdown or 10 mm. Stress-strain curves of Figure 10 shows that the separator of the invention appeared as

less rigid and less ductile than the cellulose and the Al_2O_3-coated PE separators. This was probably caused by the microstructure of the separator of the invention, made of alternated domain of semi-crystalline PVDF-HFP and SiO_2. It exhibits a tensile strength of 4.7 MPa and an elongation-at-break of 63%, while the tensile strength was reduced to 3.3 MPa and an elongation-at-break of 20% for the commercial separator (Al_2O_3-coated PE) and respectively to 5.6 MPa and 5.1% for the cellulose one (see the table below). The mechanical properties could thus be seriously modified with the nanostructure of the separator.

Separator	Strength (Mpa)	Elongation (%)	Young modulus (Mpa)
Al_2O_3-coated-PE	24.0 ± 0.6	19.9 ± 0.8	120 ± 7
Cellulose	22.5 ± 0.4	6.9 ± 0.9	326 ± 48
Separator of the invention	4.7 ± 0.4	66.8 ± 3.2	7.03 ± 0.09

Finally, the electrochemical performances of the Na-ion batteries comprising the Al_2O_3-coated PE separator, the cellulose separator and the separator according to the invention was examined in a NVPF/separator/HC full cell (Figure 11).

NVPF/separator/HC full cell comprising those two commercial separators were obtained following the same protocol as described in example 2.

Figures 11, 12 and 13 show the voltage curves of full cell with Al_2O_3-coated PE separator, cellulose separator and separator of the invention, respectively, cycled between 2 and 4.3 V at C/10 rate. The observed irreversible capacity of 9 $mAh.g^{-1}$, 21 $mAh.g^{-1}$ and 21 $mAh.g^{-1}$ respectively for Al_2O_3-coated PE separator, cellulose separator and separator of the invention, between the first charge and discharge, comes from the anode. This phenomenon corresponds to the irreversible capacity loss of the HC electrode, caused by the formation of solid electrolyte interface (SEI) film consuming Na ions irreversibly. If the reversibility is similar for each system, it reveals that the cell made with the separator of the invention exhibits a higher initial capacity of 129 $mAh.g^{-1}$ (based on the weight of cathode).

The capacity rate and thus power performance behavior of the three different cells were also studied. For these experiments, the cell was charge until 4 V, and then discharge with different capacity rates, from 5 C to C/20 with relaxation between each, until the complete discharge of the cell (Figures 14, 15 and 16). Na-ion battery containing the separator of the invention exhibits the higher capacity at 5 C discharge, revealing the

better power behavior of this system. Both properties, high specific capacity and good capacity retention at high capacity rate, can be assigned to the higher ionic conductivity of the separator of the invention, its excellent wettability and its probable electrolyte retention at the interface allowing to enhance charge transfer at high rate.

The quality of the electrode/electrolyte interfaces was then investigated by electrochemical impedance spectroscopy in symmetric Na/Na cell prepared with the three impregnated separators and the corresponding Nyquist plots are shown in Figure 17. It can be seen that the diameter of the high frequency semicircle for the cell with the separator corresponding to the invention is lower than that of the two cells including cellulose separator and Al_2O_3-coated PE separator, indicating that interfaces are considerably optimized in cell with separator of the invention.

To examine the formation of dendrites with reasonable time frames, a current density of 0.3 $mA.cm^{-2}$ has been applied on symmetric Na-Na cells to accelerate the dendrite growth (Figure 18). For commercial separator (Al_2O_3-coated PE), the voltage between the two electrodes (E_{Na-Na}) is initially 56 mV and decreases up to 50 mV due to charging effect. An increase of the voltage is then observed, probably linked to the formation of SEI layer. Finally, a sudden drop of E_{Na-Na} to nearly zero occurs for t = 30 h, which corresponds to the apparition of short circuit caused by the penetration of separator by dendrites as it has been proposed before. Similar behavior is observed for cellulose separator tested in the same condition but with short circuit time much longer (60 h). For the separator of the invention, a small drop of potential is first observed and rapidly the E_{Na-Na} increases up to the sudden E_{Na-Na} drop for t = 100 h.

CLAIMS

1. A battery separator comprising monophasic non-woven hybrid nanofibers, wherein:
- said non-woven hybrid nanofibers comprise at least one metal oxide and at least one polymer chosen from the group consisting of fluoropolymers, vinylpolymers, polyethers and mixtures thereof, and
- said non-woven hybrid nanofibers have a diameter ranging from 20 to 1,000 nm.

2. The battery separator according to claim 1, wherein the metal oxide is selected from the group consisting of SiO_2, Al_2O_3, ZrO_2, TiO_2, and mixtures thereof.

3. The battery separator according to claim 1 or 2, wherein the polymer is chosen from the group consisting of polyvinylidene fluoride (PVDF), polyvinylidene fluoride-hexafluoropropylene (PVDF-HFP), polyethylene oxide (PEO), polyvinylpyrrolidone (PVP), polyvinyl alcohol (PVA) and mixtures thereof.

4. The battery separator according to any of claims 1 to 3, wherein the metal oxide content ranges from 5% to 70% by weight in relation to the total weight of non-woven hybrid nanofibers.

5. The battery separator according to any of claims 1 to 4, wherein the polymer content ranges from 30% to 95% by weight in relation to the total weight of non-woven hybrid nanofibers.

6. The battery separator according to any of claims 1 to 5, having a thickness ranging from 10 µm to 100 µm.

7. The battery separator according to any of claims 1 to 6, having a porosity ranging from 10% to 90% by volume in relation to the total volume of said battery separator.

8. A process for manufacturing the battery separator according to any of claims 1 to 7, said process coupling a sol-gel reaction and an electrospinning method, comprising the following steps:
i) preparing a mixture comprising at least one polymer as defined in claim 1 and one metal precursor, said metal precursor being a metal alkoxide chosen from the

group consisting of silicon alkoxide, titanium alkoxide, zirconium alkoxide and aluminum alkoxide,

ii) electrospinning the mixture obtained at the end of step i) by applying a positive voltage to said mixture for obtaining a material deposited onto a support, and

iii) drying the deposited material obtained at the end of step ii) and removing the support to obtain the battery separator.

9. The process according to claim 8, wherein the metal precursor is chosen from the group consisting of tetraethyl orthosilicate, titanium tetraisopropoxide, zirconium tetraisopropoxide, aluminium isopropoxide and mixtures thereof.

10. The process according to claim 8 or 9, wherein the mixture of step i) is prepared in a solvent chosen from the group consisting of N,N-dimethylformamide, ethanol, tetrahydrofuran, and mixtures thereof.

11. The process according to any of claims 8 to 10, wherein the positive voltage applied during step ii) is comprised between 5 and 25 kV.

12. The use of the battery separator according to any of claims 1 to 7, in a Li-ion battery, Na-ion battery or metal-air battery.

13. A Na-ion battery comprising:

- at least one positive electrode comprising at least one positive electrode active material and a current collector,
- at least one negative electrode comprising a negative electrode active material, and
- at least one battery separator according to any of claims 1 to 7, said battery separator being impregnated with at least one electrolyte and being placed between the positive electrode and the negative electrode.

14. The Na-ion battery according to claim 13, wherein the electrolyte comprises at least one solvent chosen from the group consisting of ethylene carbonate-dimethyl carbonate (EC-DMC), ethylene carbonate-propylene carbonate (EC-PC),water in salt, and mixtures thereof, and at least one sodium salt.

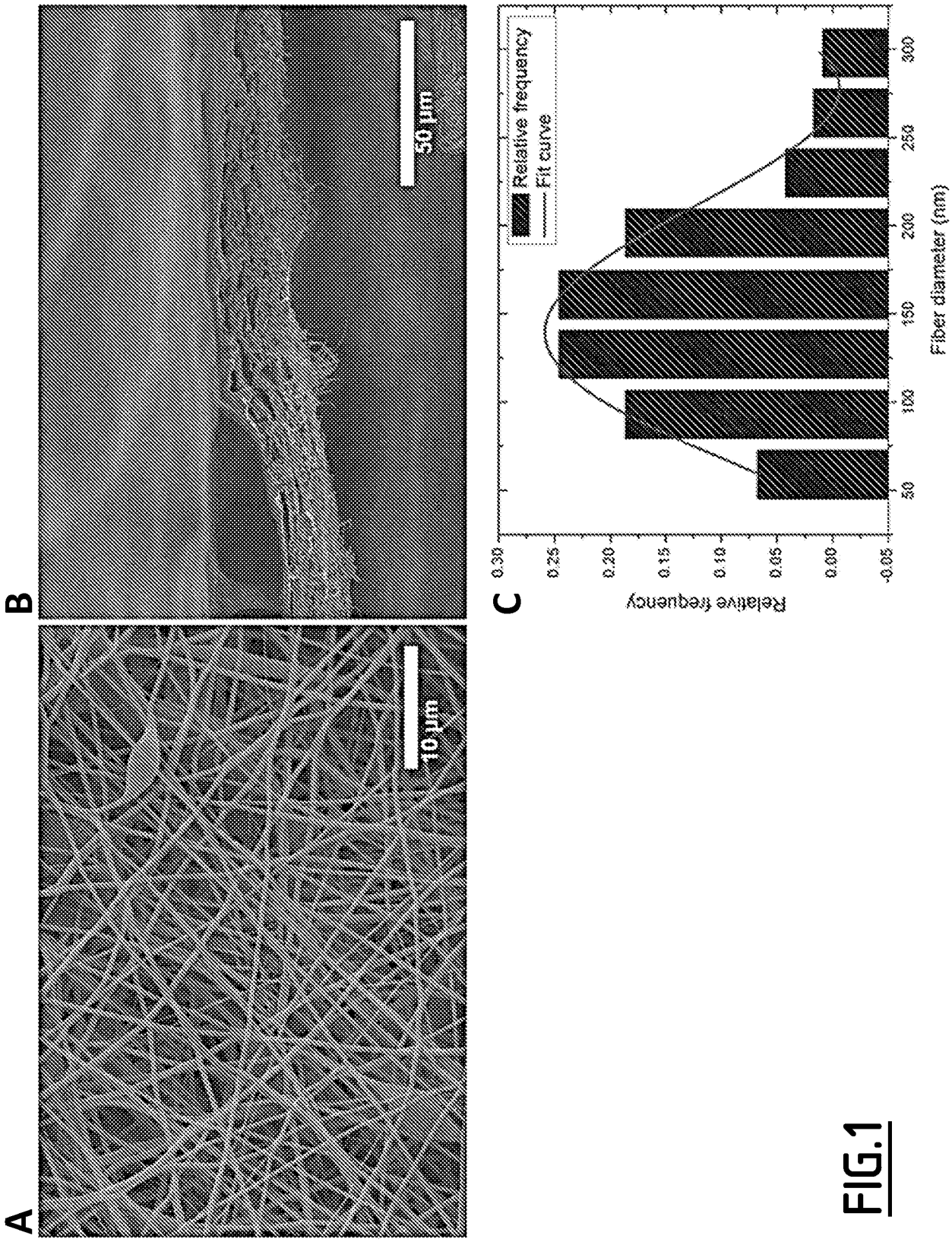

A
10 µm
B
50 µm
C
Relative frequency
Fit curve
0.30
0.25
0.20
0.15
0.10
0.05
0.00
-0.05
50
100
150
200
250
300
Fiber diameter (nm)

FIG.1

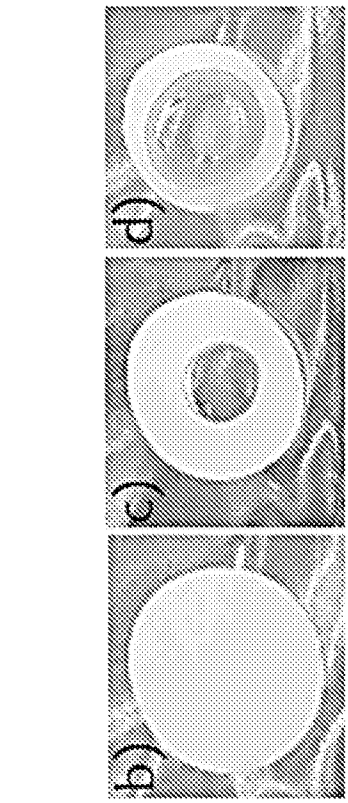


FIG.2

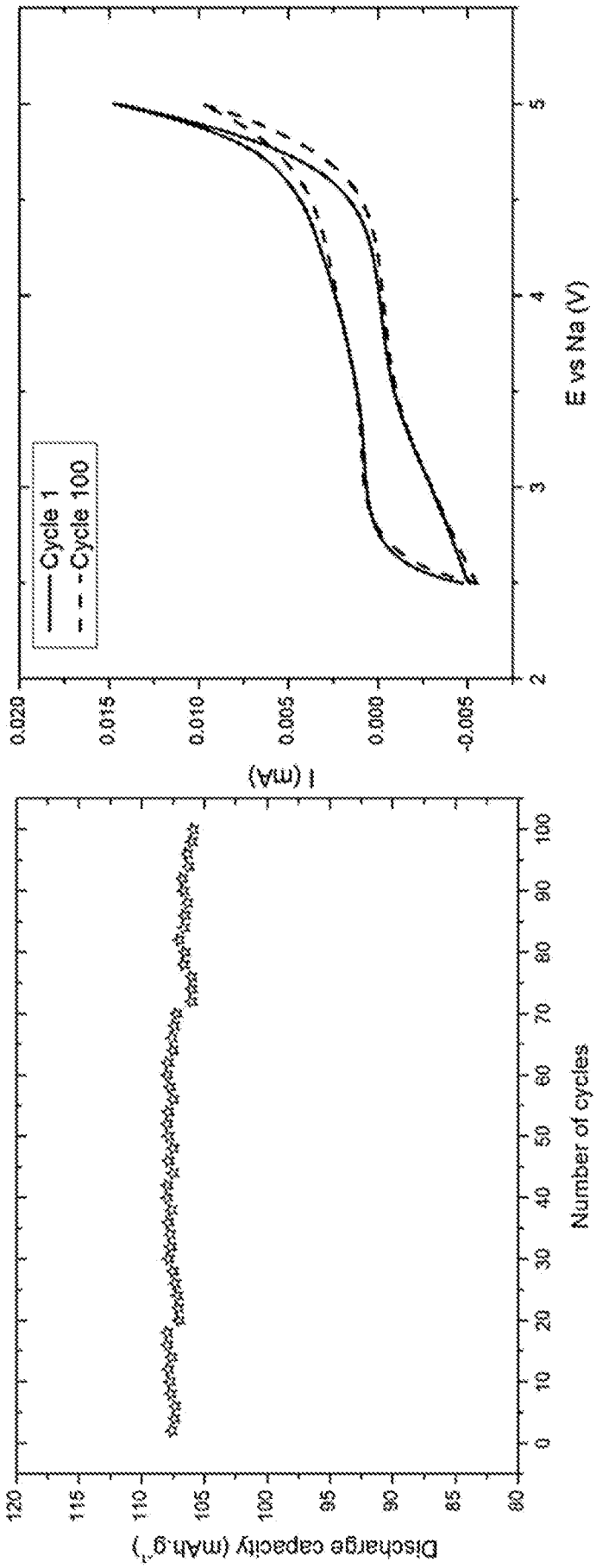

Discharge capacity (mAh.g-1)
Number of cycles
I (mA)
E vs Na (V)
Cycle 1
Cycle 100

FIG.3

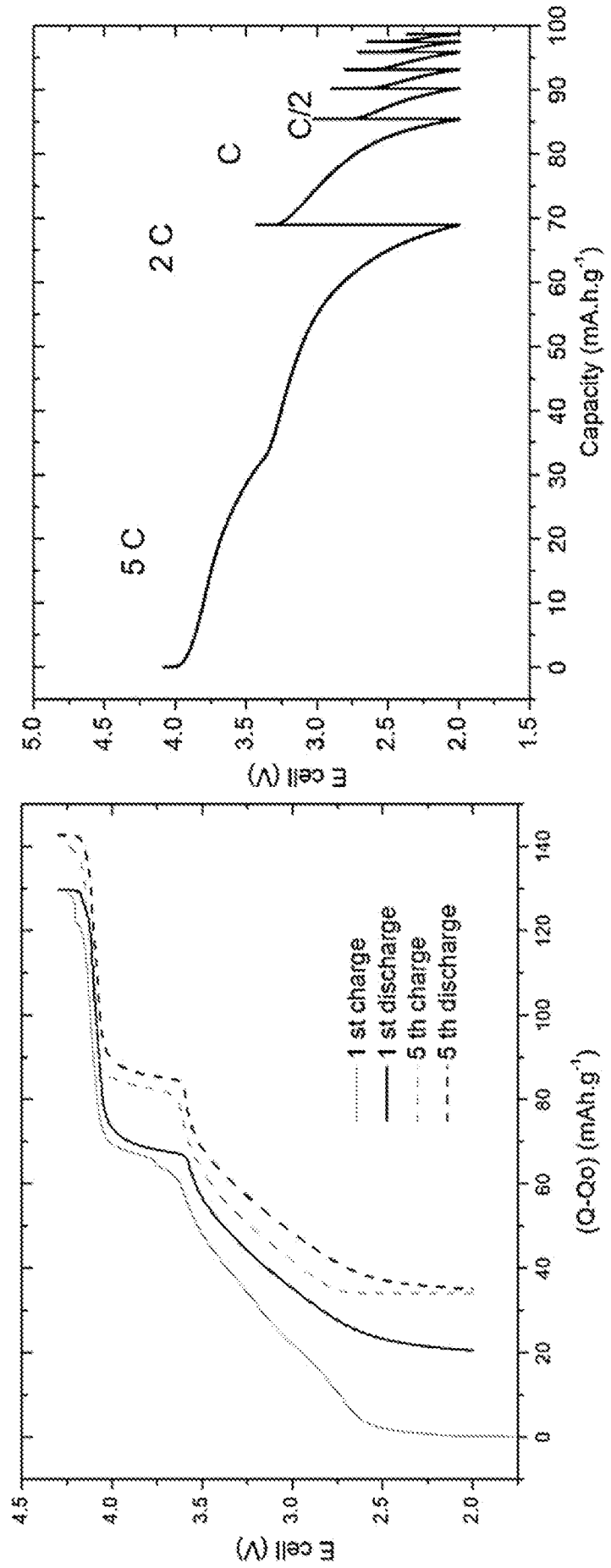

E cell (V)
Capacity (mA.h.g-1)
5 C
2 C
C
C/2
E cell (V)
(Q-Qo) (mAh.g-1)
1 st charge
1 st discharge
5 th charge
5 th discharge

FIG.4

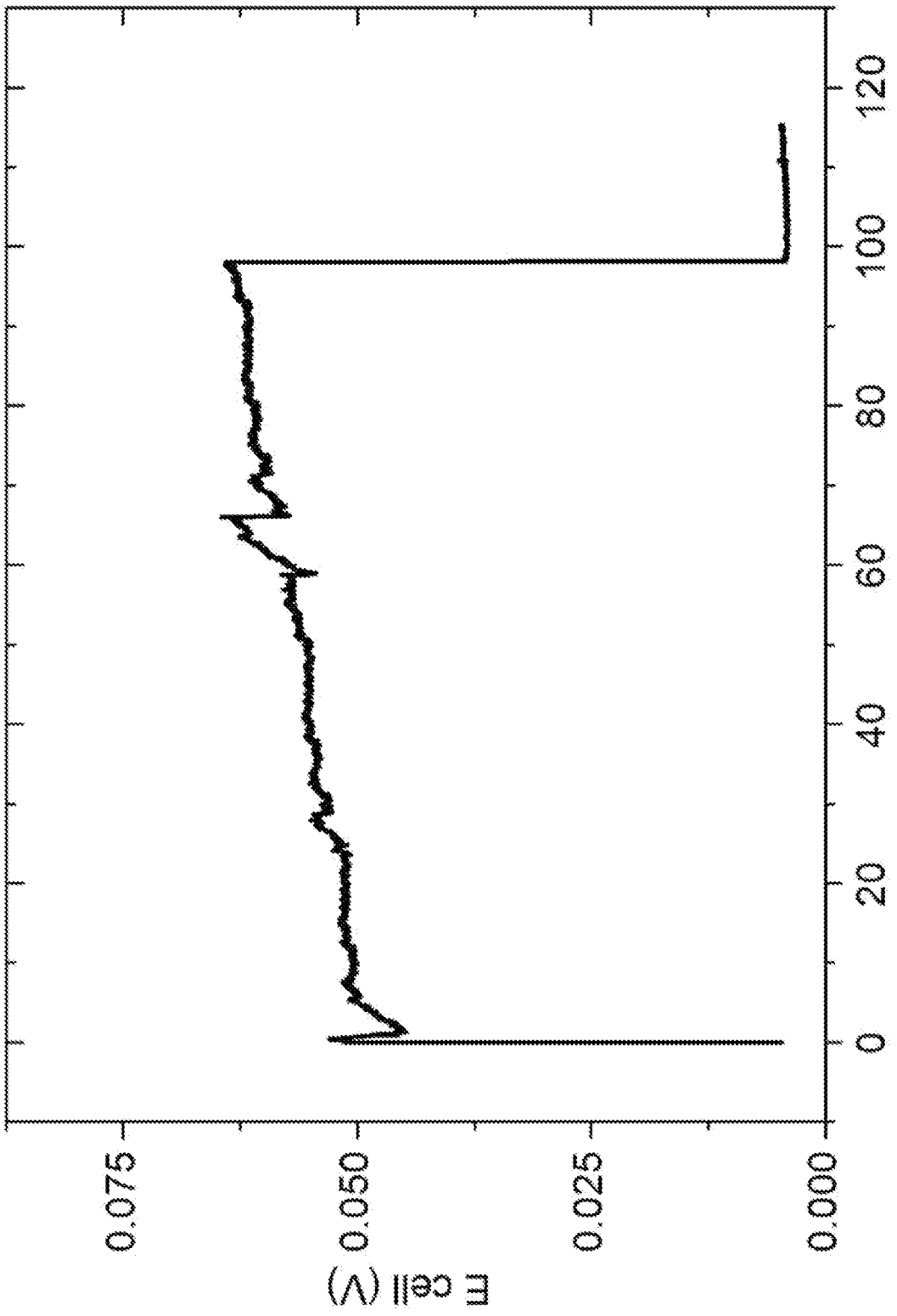


FIG.5

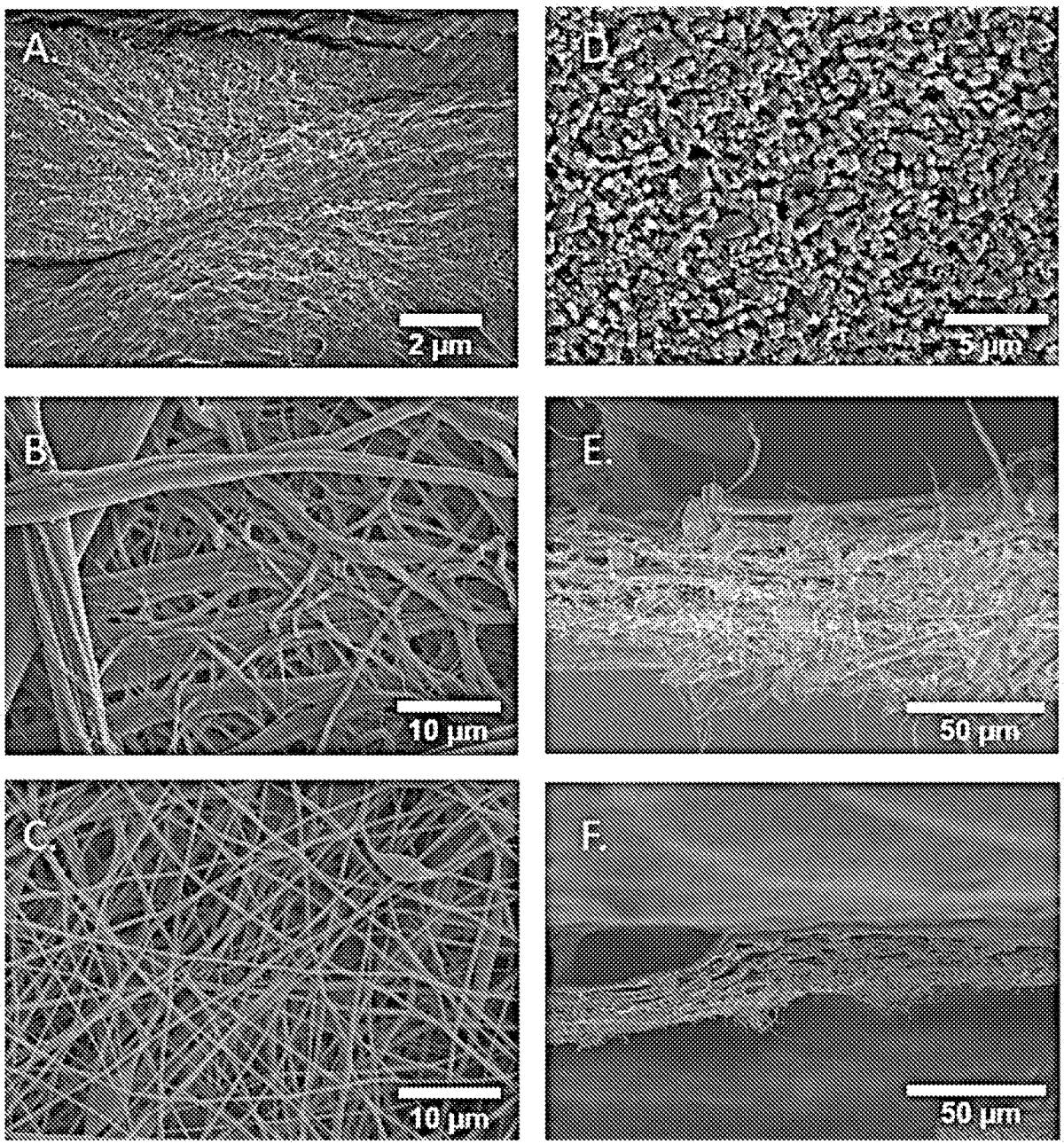


FIG.6

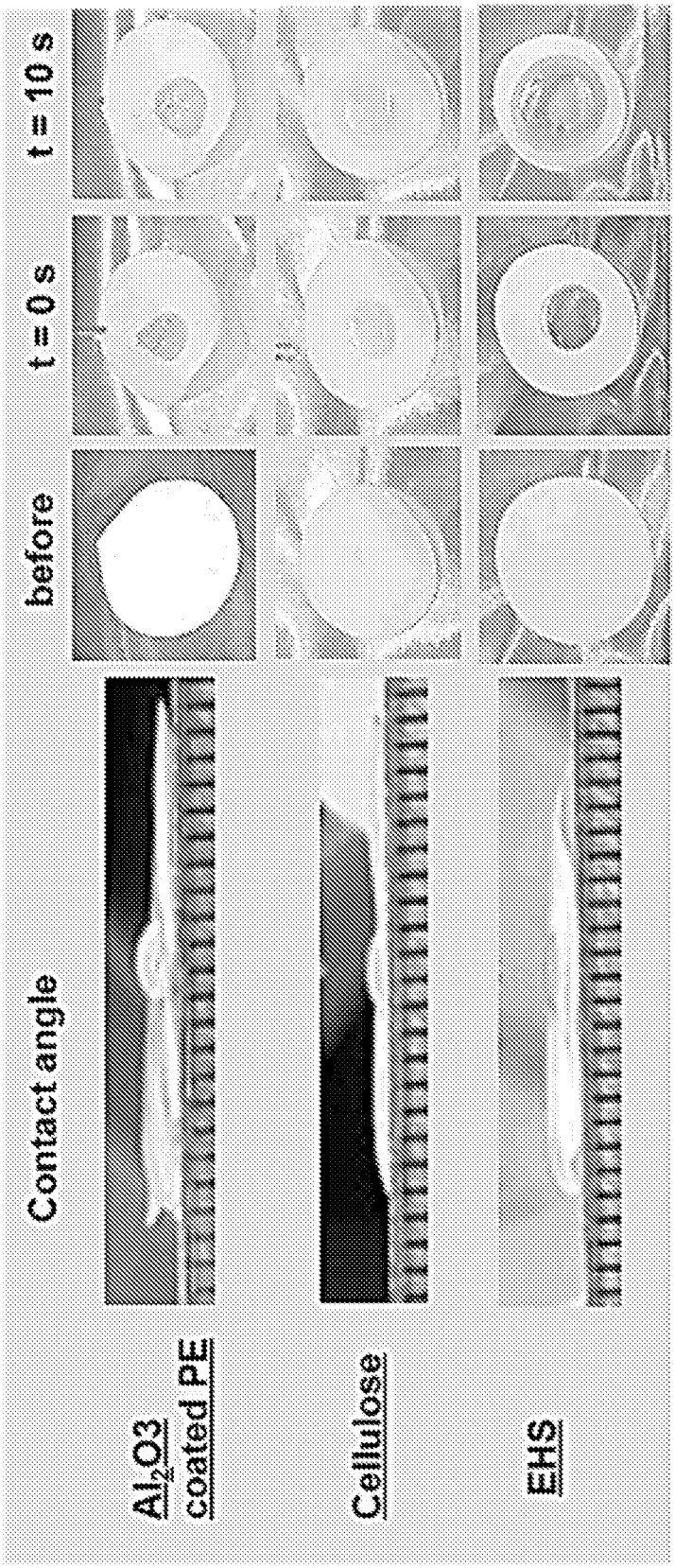

Contact angle
before
t = 0 s
t = 10 s
Al2O3 coated PE
Cellulose
EHS

FIG.7

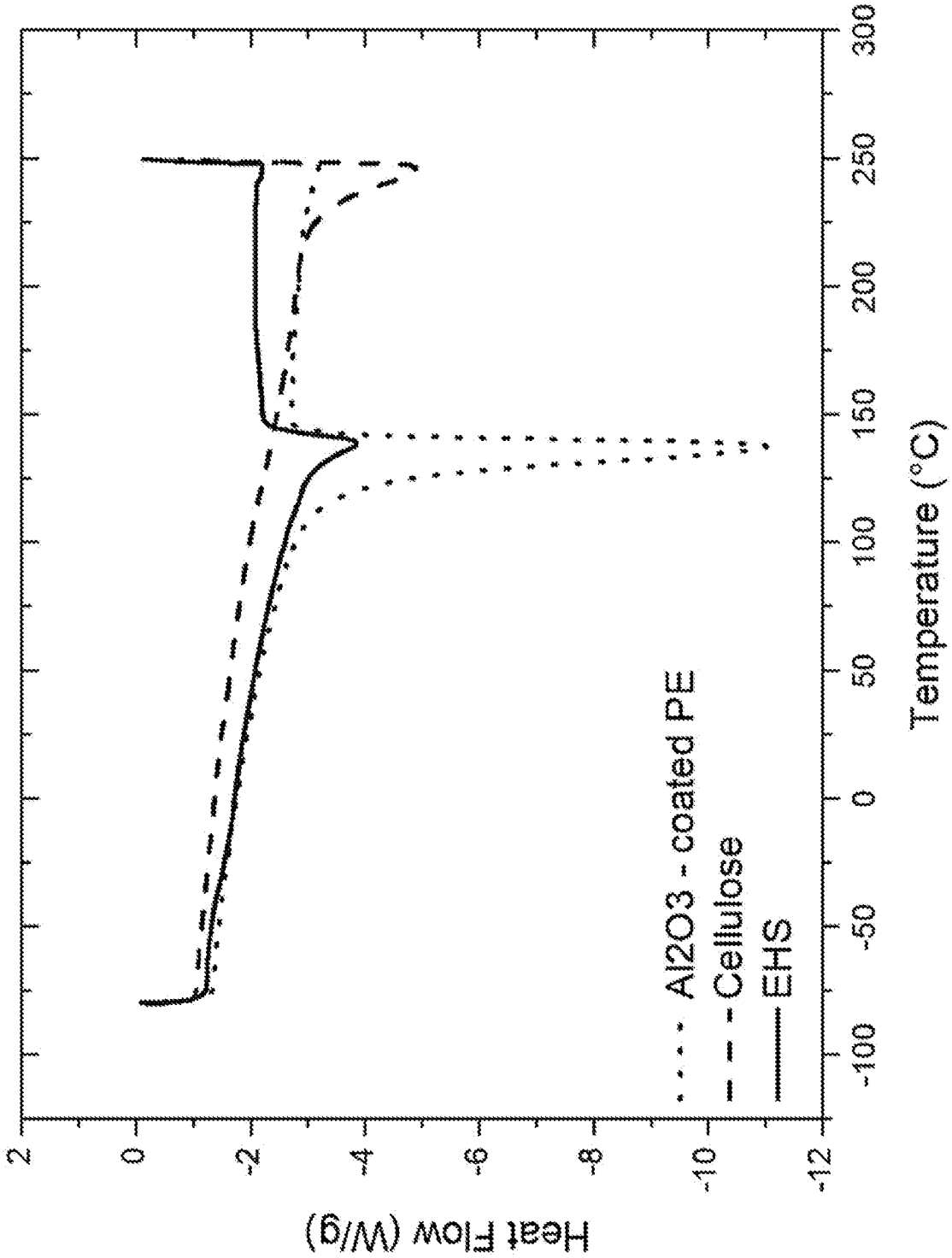

Heat Flow (W/g)
2
0
-2
-4
-6
-8
-10
-12
Temperature (°C)
-100
-50
0
50
100
150
200
250
300
Al2O3 - coated PE
Cellulose
EHS

FIG.8

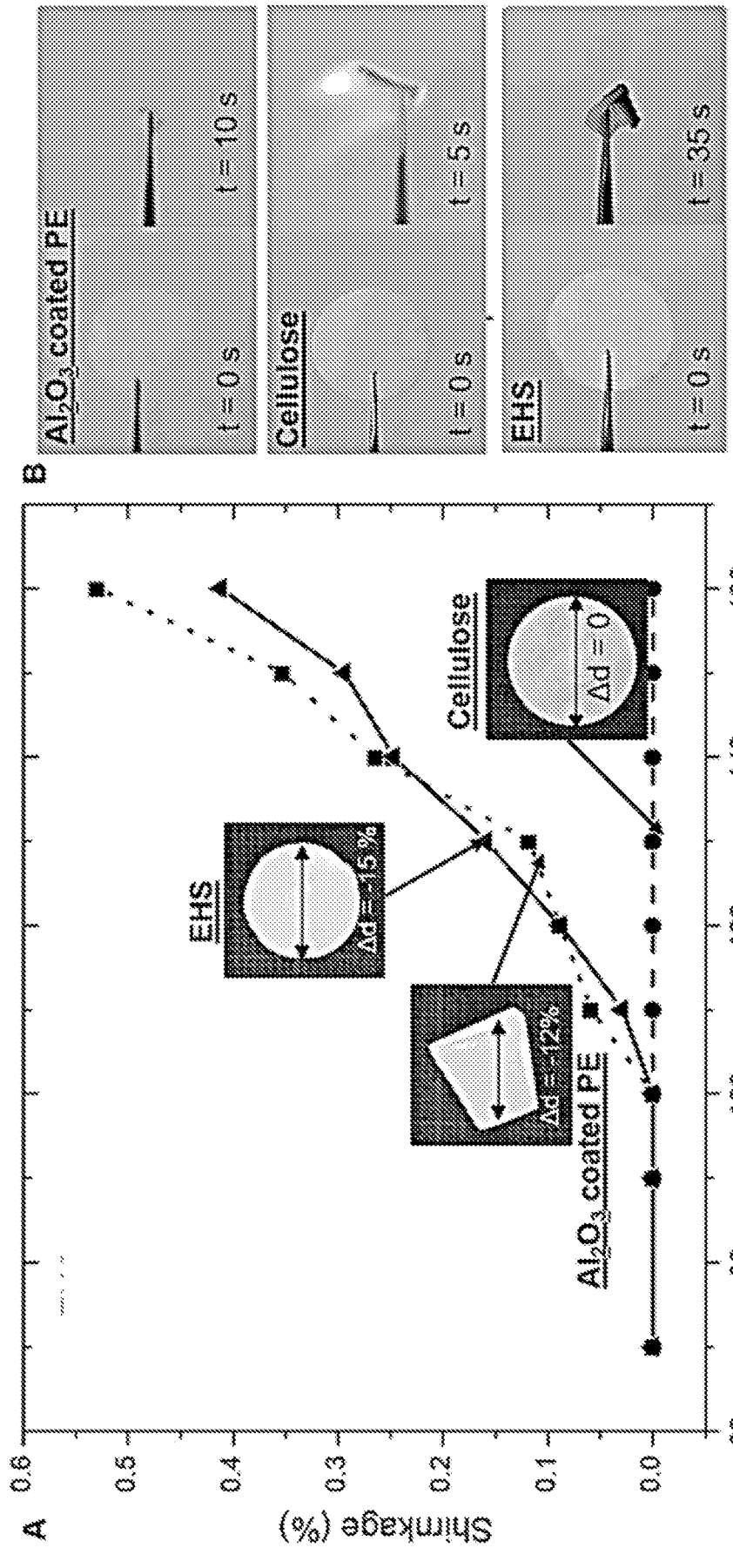

A
B
Shrinkage (%)
Temperature (°C)
0.0
0.1
0.2
0.3
0.4
0.5
0.6
60
80
100
120
140
160
EHS
Δd = 16 %
Cellulose
Δd = 0
Al2O3 coated PE
Δd = 12%
Al2O3 coated PE
t = 0 s
t = 10 s
Cellulose
t = 0 s
t = 5 s
EHS
t = 0 s
t = 35 s

FIG.9

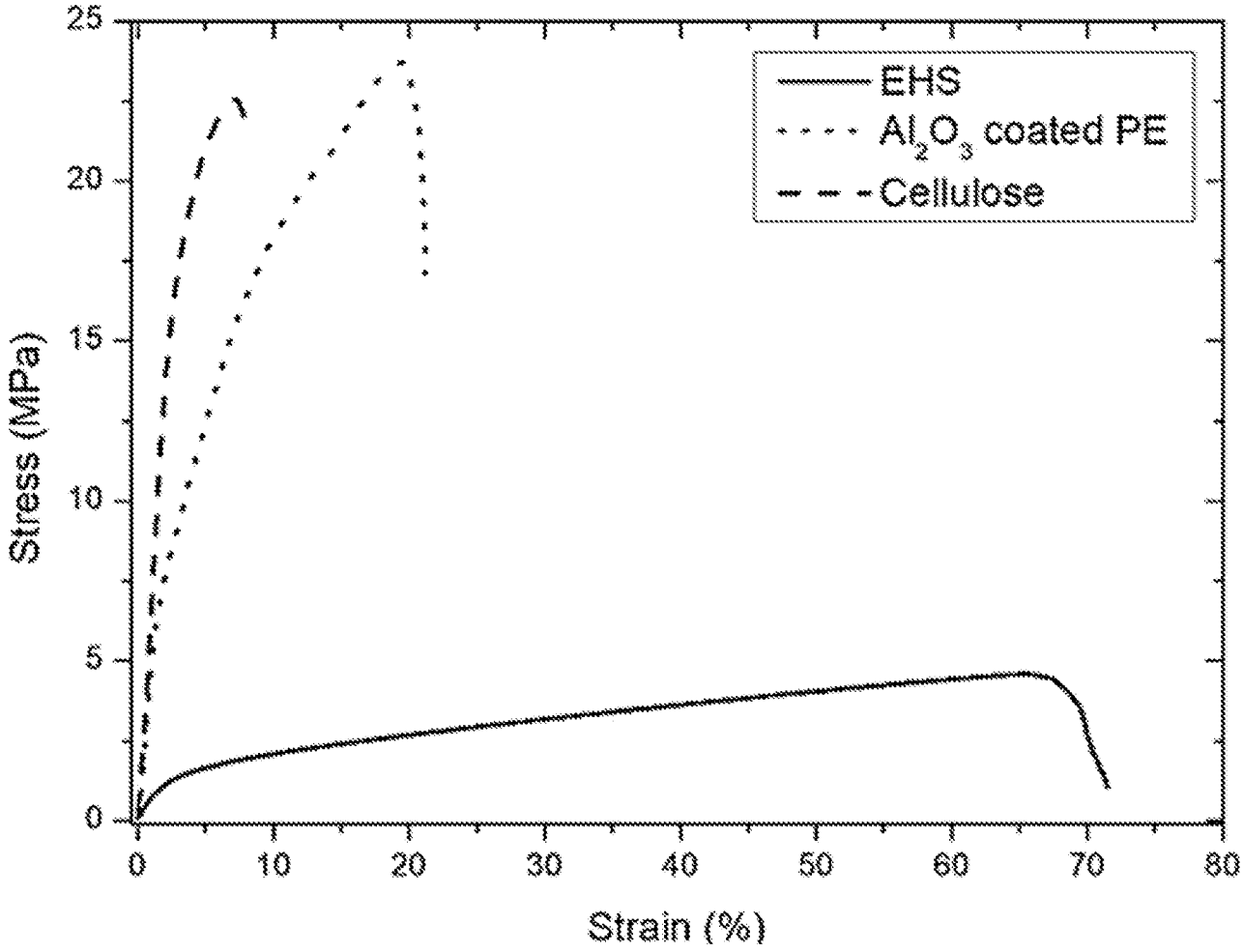

EHS
Al_2O_3 coated PE
Cellulose
Stress (MPa)
Strain (%)
0
5
10
15
20
25
0
10
20
30
40
50
60
70
80

FIG.10

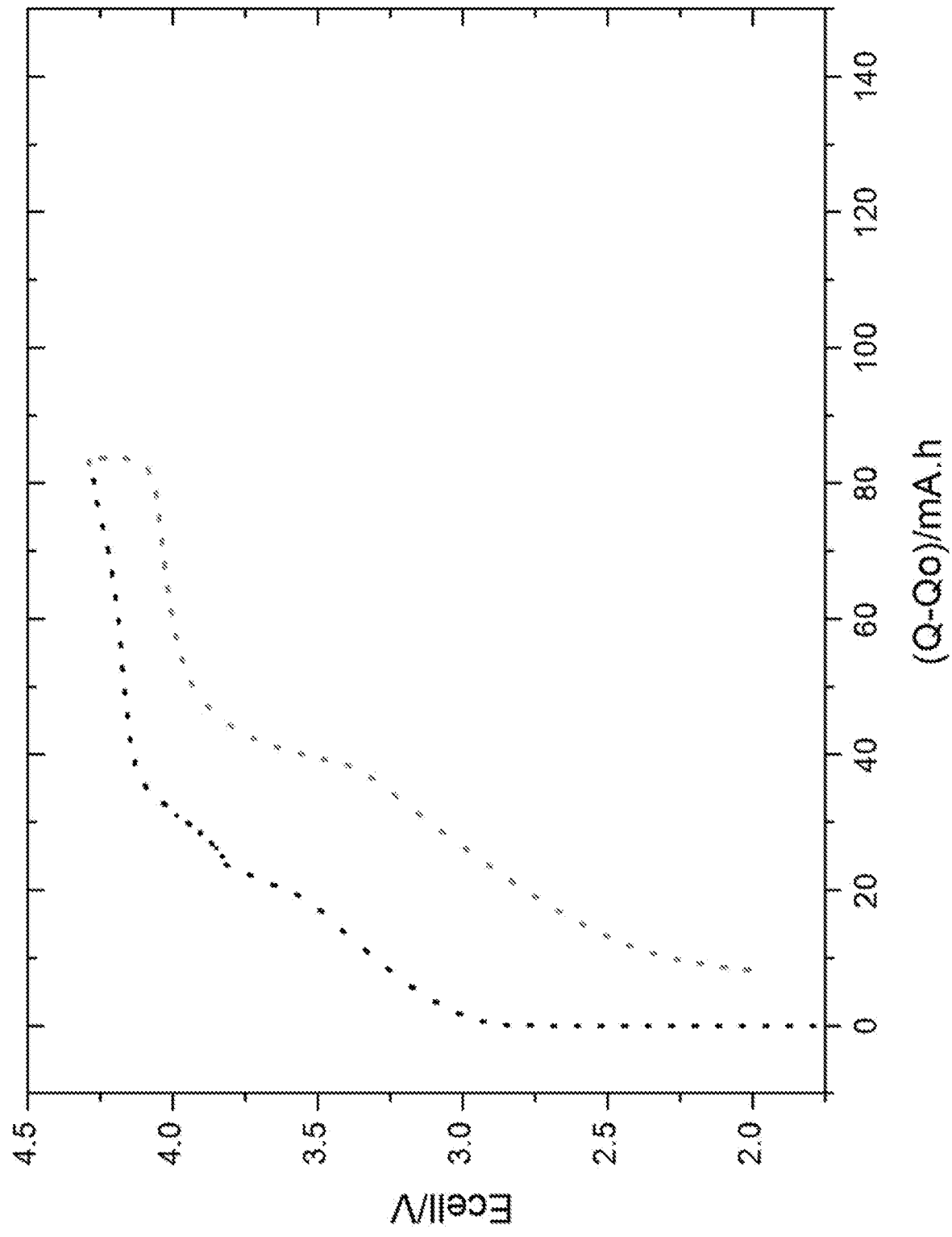


FIG.11

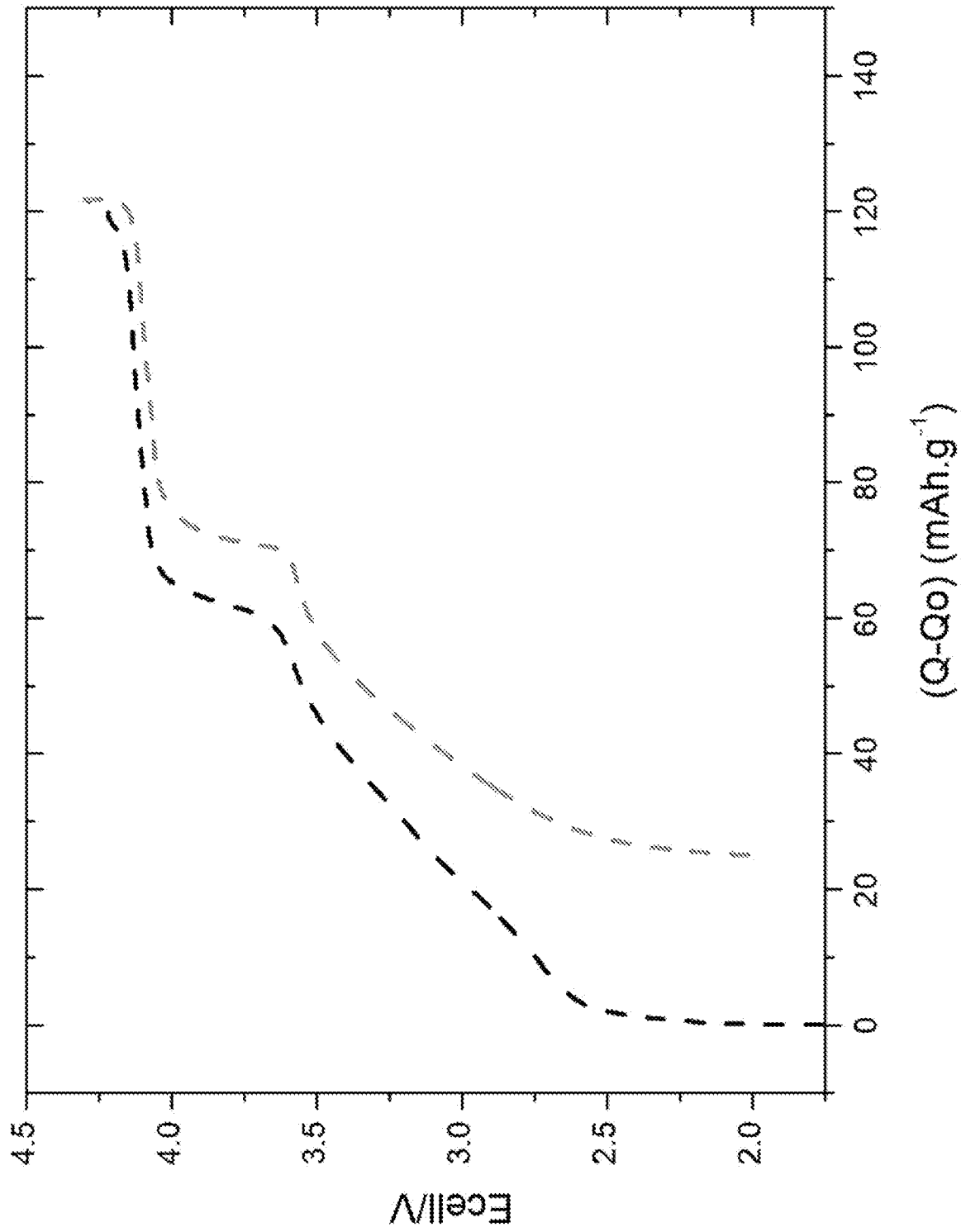


FIG.12

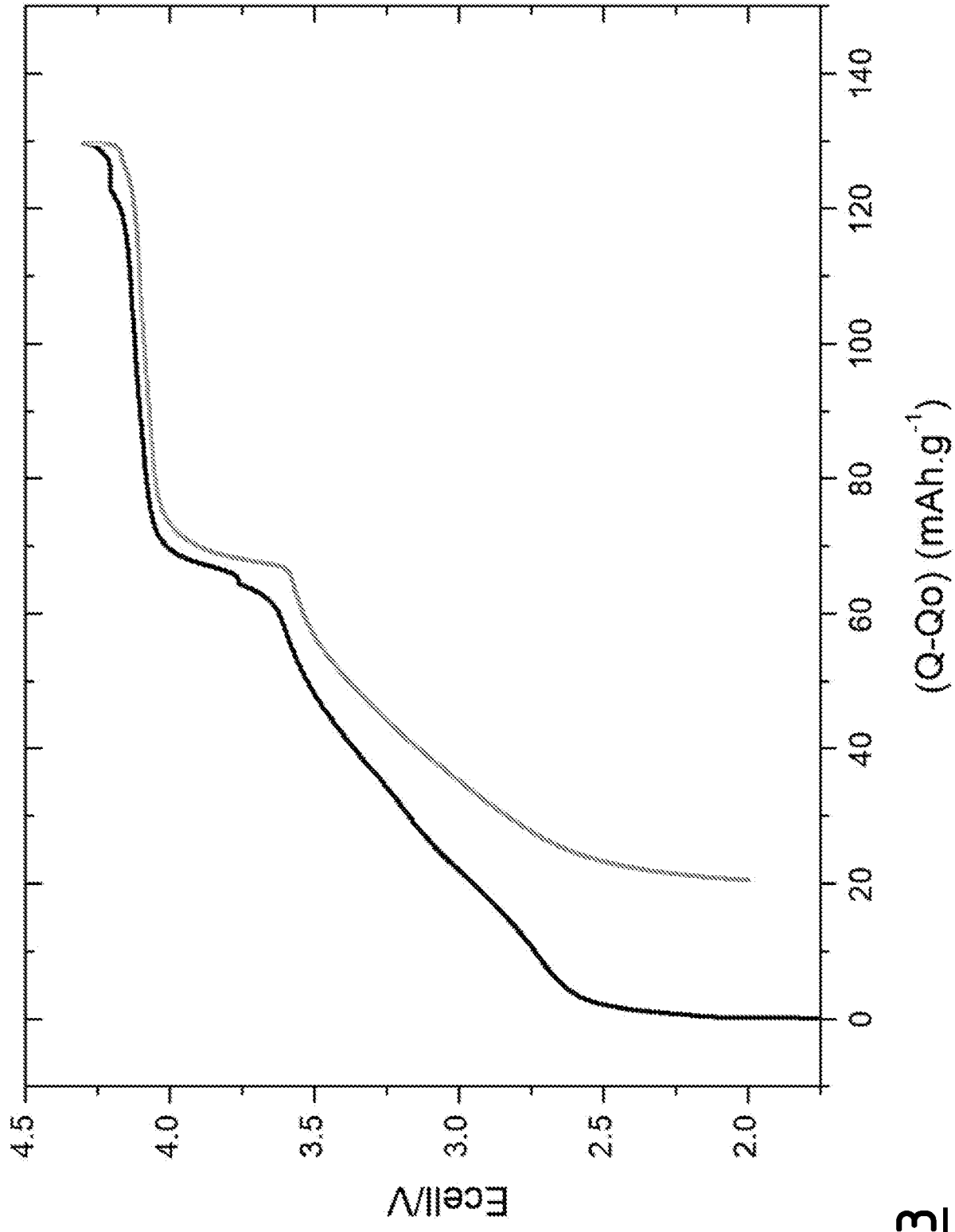


FIG.13

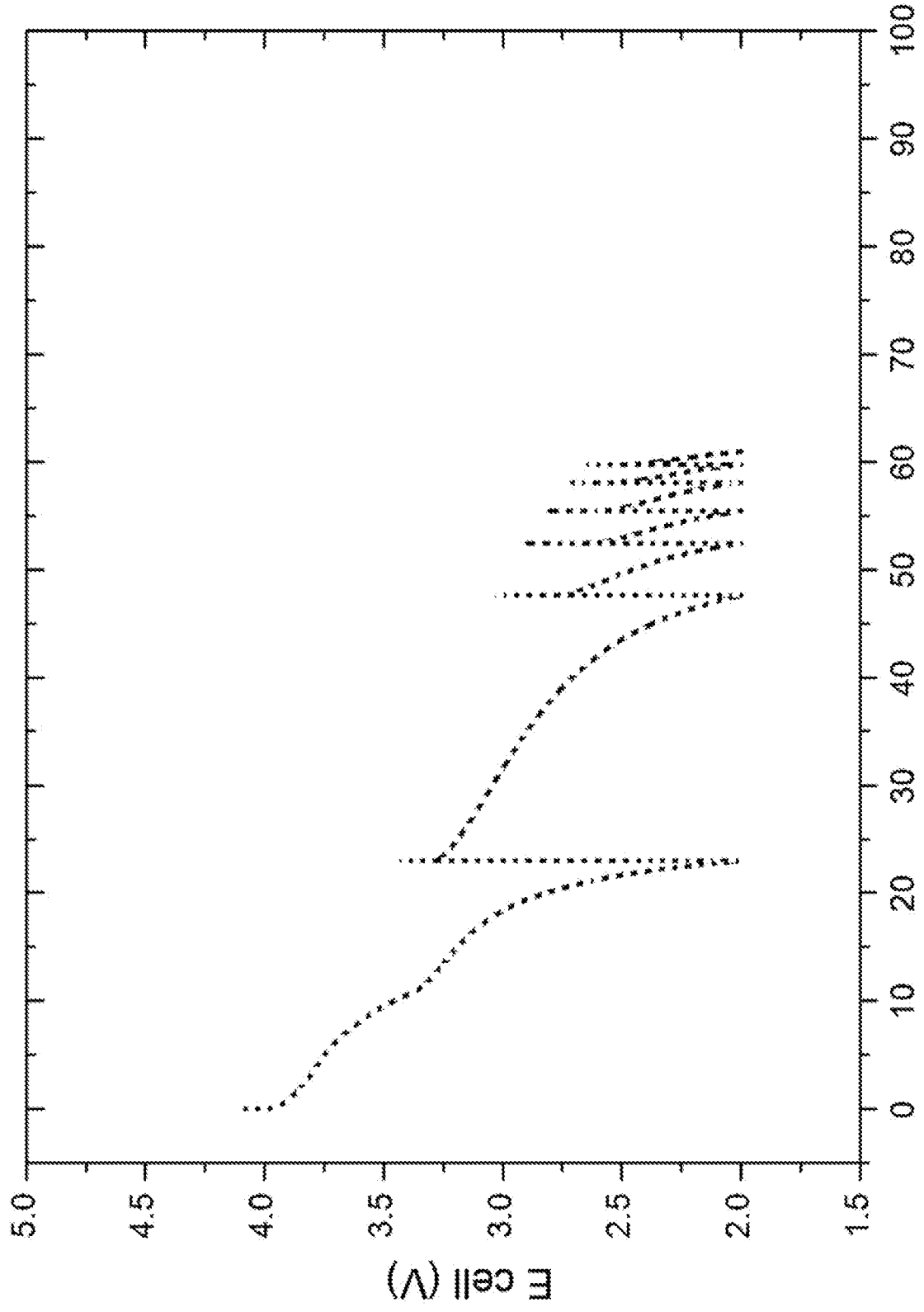

E cell (V)
5.0
4.5
4.0
3.5
3.0
2.5
2.0
1.5
0
10
20
30
40
50
60
70
80
90
100
Capacity (mA.h.g-1)

FIG.14

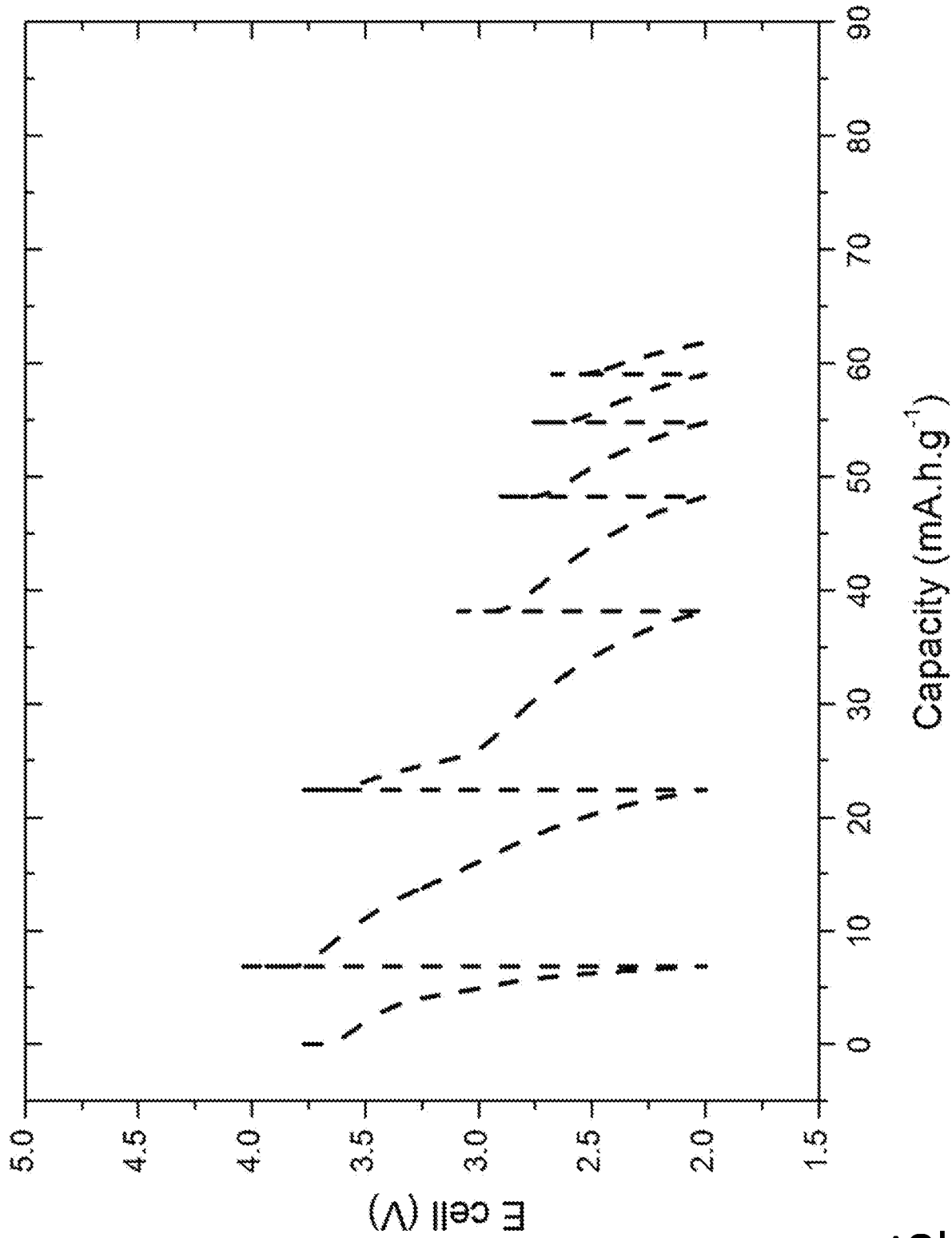

E cell (V)
5.0
4.5
4.0
3.5
3.0
2.5
2.0
1.5
0
10
20
30
40
50
60
70
80
90
Capacity (mA.h.g-1)

FIG.15

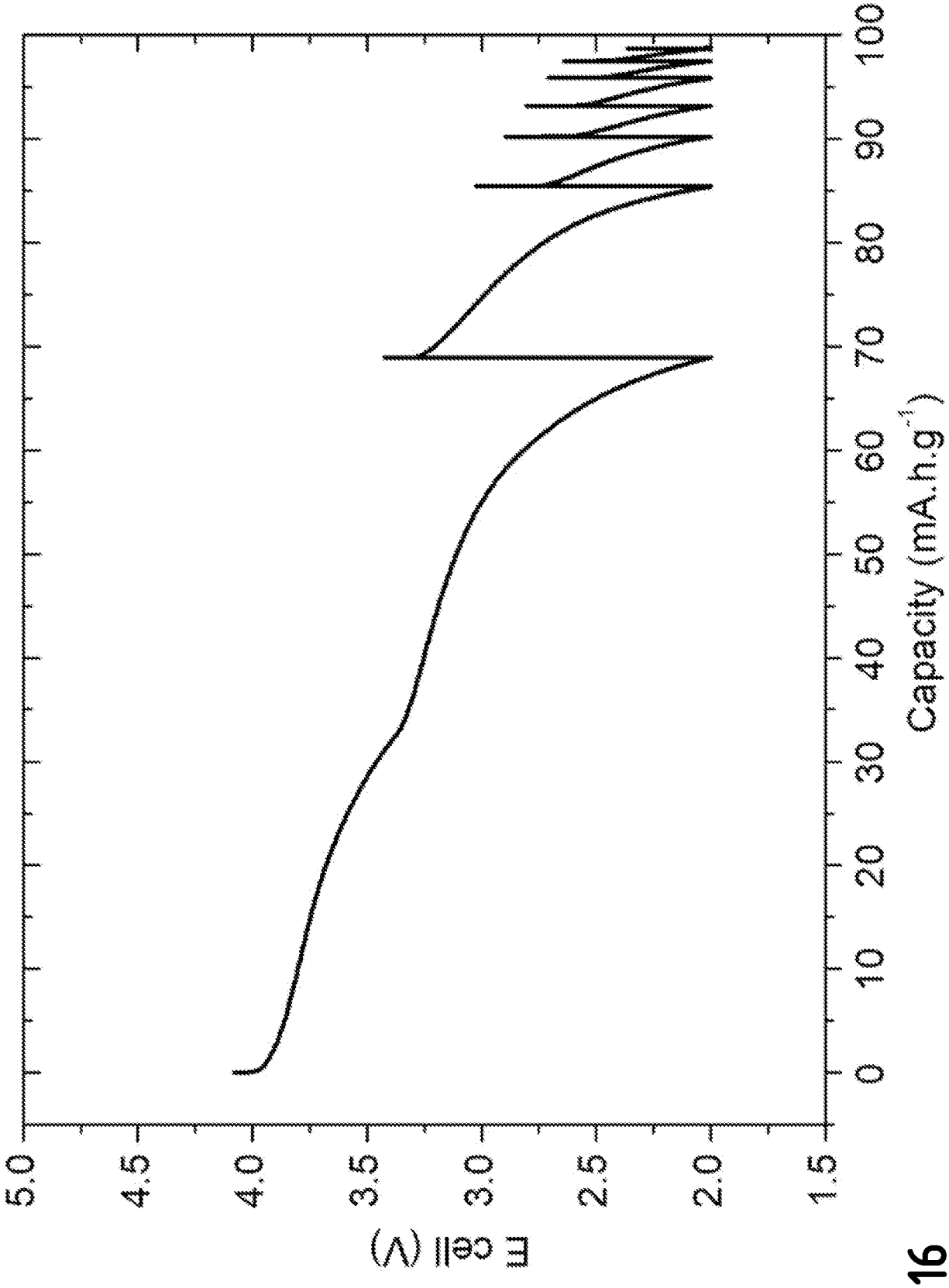

E cell (V)
5.0
4.5
4.0
3.5
3.0
2.5
2.0
1.5
0
10
20
30
40
50
60
70
80
90
100
Capacity (mA.h.g-1)

FIG.16

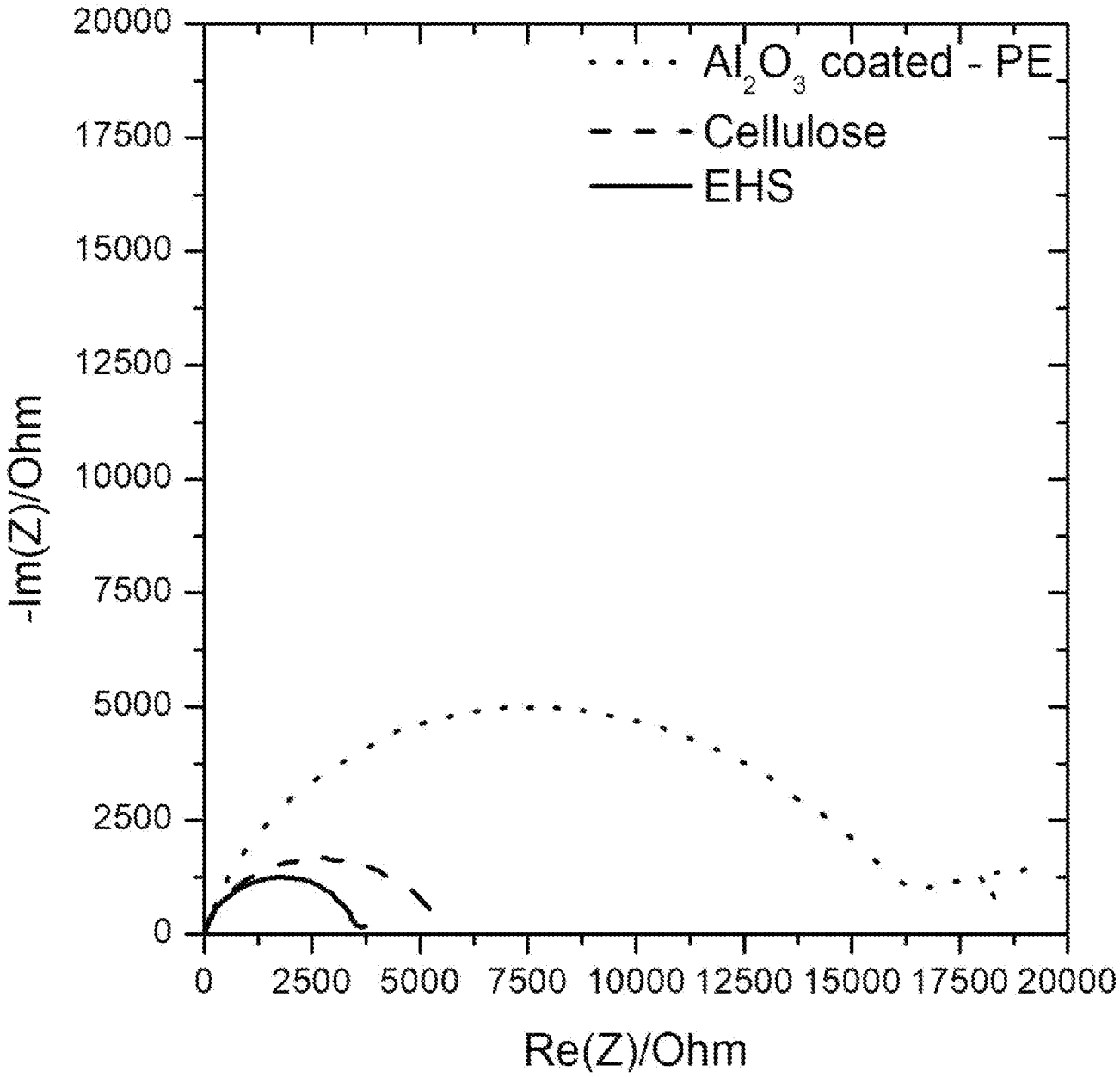

20000
17500
15000
12500
10000
7500
5000
2500
0
-Im(Z)/Ohm
0
2500
5000
7500
10000
12500
15000
17500
20000
Re(Z)/Ohm
Al2O3 coated - PE
Cellulose
EHS

FIG.17

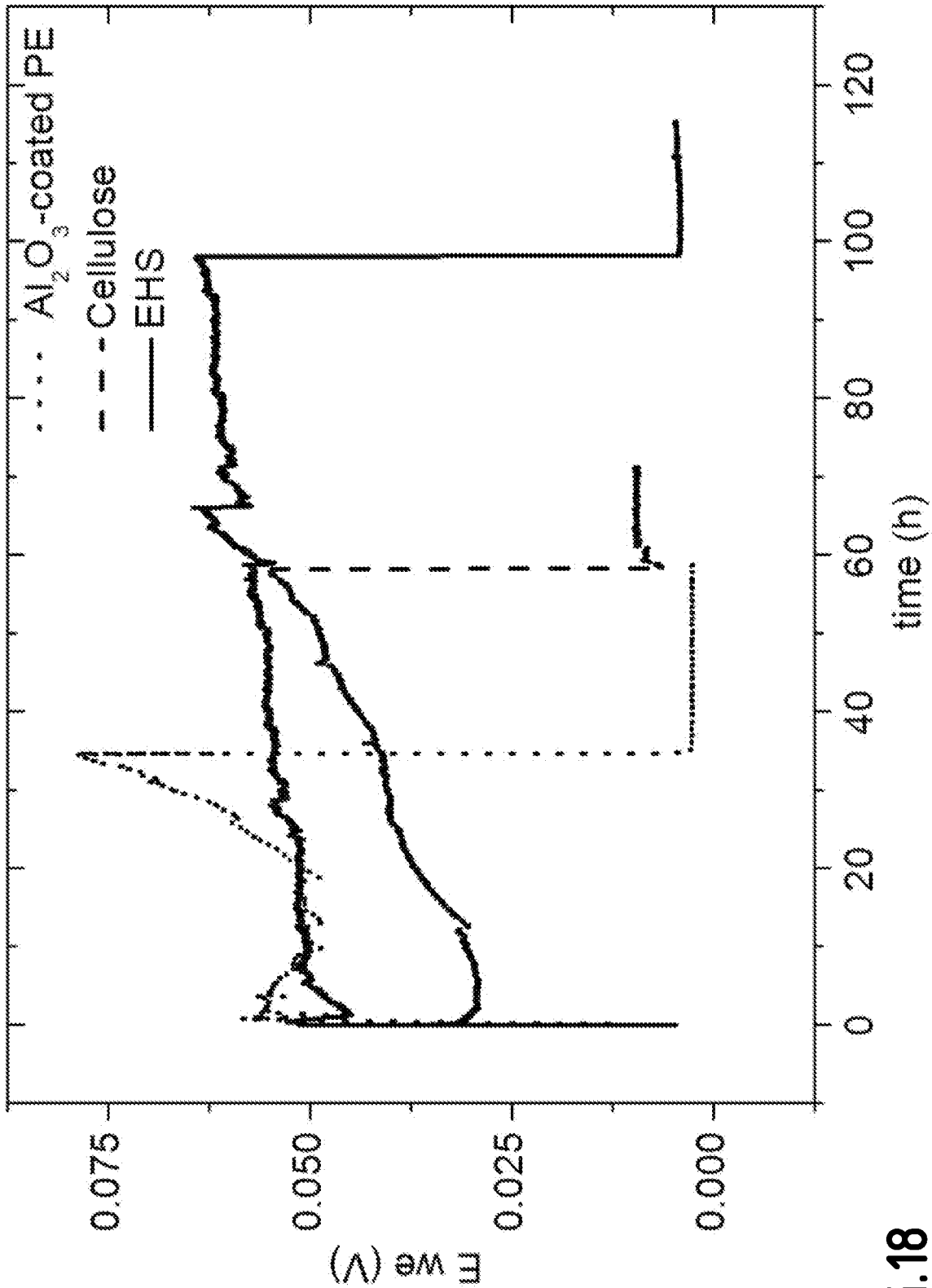

Al_2O_3-coated PE
Cellulose
EHS
E we (V)
0.000
0.025
0.050
0.075
0
20
40
60
80
100
120
time (h)

FIG.18

INTERNATIONAL SEARCH REPORT

International application No
PCT/IB2019/000452

A. CLASSIFICATION OF SUBJECT MATTER
INV. H01M2/14 H01M2/16
ADD.

According to International Patent Classification (IPC) or to both national classification and IPC

B. FIELDS SEARCHED

Minimum documentation searched (classification system followed by classification symbols)
H01M

Documentation searched other than minimum documentation to the extent that such documents are included in the fields searched

Electronic data base consulted during the international search (name of data base and, where practicable, search terms used)
EPO-Internal, WPI Data

C. DOCUMENTS CONSIDERED TO BE RELEVANT

Category*	Citation of document, with indication, where appropriate, of the relevant passages	Relevant to claim No.
X	US 2012/082884 A1 (ORILALL MAHENDRA C [US] ET AL) 5 April 2012 (2012-04-05) claims 1-20 paragraph [0040] -----	1-14
X	WO 2014/066310 A1 (UNIV CORNELL [US]) 1 May 2014 (2014-05-01) paragraphs [0038], [0042], [0054], [0069], [0094] - [0098] paragraphs [0068], [0075] -----	1-14
X	US 2015/318570 A1 (CHOI WON GIL [KR] ET AL) 5 November 2015 (2015-11-05) paragraphs [0050], [0058] - [0063], [0082] -----	1-14

-/--

[X] Further documents are listed in the continuation of Box C.

[X] See patent family annex.

* Special categories of cited documents :

"A" document defining the general state of the art which is not considered to be of particular relevance

"E" earlier application or patent but published on or after the international filing date

"L" document which may throw doubts on priority claim(s) or which is cited to establish the publication date of another citation or other special reason (as specified)

"O" document referring to an oral disclosure, use, exhibition or other means

"P" document published prior to the international filing date but later than the priority date claimed

"T" later document published after the international filing date or priority date and not in conflict with the application but cited to understand the principle or theory underlying the invention

"X" document of particular relevance; the claimed invention cannot be considered novel or cannot be considered to involve an inventive step when the document is taken alone

"Y" document of particular relevance; the claimed invention cannot be considered to involve an inventive step when the document is combined with one or more other such documents, such combination being obvious to a person skilled in the art

"&" document member of the same patent family

Date of the actual completion of the international search	Date of mailing of the international search report
14 October 2019	25/10/2019

Name and mailing address of the ISA/	Authorized officer
European Patent Office, P.B. 5818 Patentlaan 2 NL - 2280 HV Rijswijk Tel. (+31-70) 340-2040, Fax: (+31-70) 340-3016	Haering, Christian

INTERNATIONAL SEARCH REPORT

International application No
PCT/IB2019/000452

C(Continuation). DOCUMENTS CONSIDERED TO BE RELEVANT

Category*	Citation of document, with indication, where appropriate, of the relevant passages	Relevant to claim No.
X	US 2012/003524 A1 (JO SEONG MU [KR] ET AL) 5 January 2012 (2012-01-05) paragraphs [0017] - [0025], [0029], [0034] - [0040], [0042]	1-14
X	US 2017/263908 A1 (LAICER CASTRO [US] ET AL) 14 September 2017 (2017-09-14) paragraphs [0043], [0045], [0048], [0052] - [0056], [0060]	1-14
X	US 2015/037651 A1 (HUANG XIAOSONG [US]) 5 February 2015 (2015-02-05)	1-7, 12-14
A	paragraphs [0008], [0012], [0026], [0031] claims 1-7	8-11

INTERNATIONAL SEARCH REPORT

Information on patent family members

International application No
PCT/IB2019/000452

Patent document cited in search report	Publication date	Patent family member(s)	Publication date
US 2012082884 A1	05-04-2012	CN 103168384 A	19-06-2013
		JP 6227411 B2	08-11-2017
		JP 2013539186 A	17-10-2013
		KR 20130108594 A	04-10-2013
		TW 201230453 A	16-07-2012
		US 2012082884 A1	05-04-2012
		US 2015372271 A1	24-12-2015
		WO 2012050682 A2	19-04-2012
WO 2014066310 A1	01-05-2014	US 2015287967 A1	08-10-2015
		US 2019123321 A1	25-04-2019
		WO 2014066310 A1	01-05-2014
US 2015318570 A1	05-11-2015	CN 104919639 A	16-09-2015
		US 2015318570 A1	05-11-2015
US 2012003524 A1	05-01-2012	CN 102218271 A	19-10-2011
		KR 20110116489 A	26-10-2011
		US 2012003524 A1	05-01-2012
US 2017263908 A1	14-09-2017	US 2017263908 A1	14-09-2017
		WO 2017180264 A2	19-10-2017
US 2015037651 A1	05-02-2015	NONE	